



DRIVEMODE

Integrated Modular Distributed Drivetrain for Electric & Hybrid Vehicles

Document title: Report on considered electrical motor technologies, evaluation matrix, concept decision

D3.2: Report on considered electrical motor technologies, evaluation matrix, concept decision
WP 3, T 3.1 and T 3.2

Author: Damijan Miljavec (UL)



This project has received funding from the European Union's Horizon 2020 research and innovation programme under grant agreement N°769989



Technical references

Project Acronym	DRIVEMODE
Project Title	Integrated Modular Distributed Drivetrain for Electric & Hybrid Vehicles
Project Coordinator	Mikko Pihlatie VTT Technical Research Centre of Finland mikko.pihlatie@vtt.fi
Project Duration	November 2017 – October 2020 (36 months)
Deliverable No.	D3.2
Dissemination level*	CO
Work Package	WP 3 – E-Motor
Task	T3.1 – Concept phase, T3.2 – 3D design phase
Lead beneficiary	UL
Contributing beneficiary/ies	AVL, TeD
Due date of deliverable	30 September 2018
Actual submission date	15 November 2018

* PU = Public

PP = Restricted to other programme participants (including the Commission Services)

RE = Restricted to a group specified by the consortium (including the Commission Services)

CO = Confidential, only for members of the consortium (including the Commission Services)

v	Date	Beneficiary	Author	Beneficiary
0.1	1 July 2018	Initial draft	Damijan Miljavec	UL
0.2	30.8. 2018	First draft for review	Damijan Miljavec	UL
0.3	14 September 2018	Commented	Alexander Smirnov	VTT
0.4	18.9.2018	Updated document, general concerns high speed motor and comments of WP3 partners added		
0.5	25.9.2018	Second draft for review	Damijan Miljavec	UL



This project has received funding from the European Union's Horizon 2020 research and innovation programme under grant agreement N° 769989.



0.6	3.10.2018	Commented and minor corrections	Alexander Smirnov	VTT
0.7	10.10.2018	Added to abbreviation index and minor corrections	Damijan Miljavec	UL
0.8	16.10.2018	Commented and ASM Addition	Katrin Wand	AVL
0.9	17.10.2018	Applied the comments and finalized	Damijan Miljavec	UL
0.91	20.10.2018	TMT approved	Alexander Smirnov	VTT
1.0	15.11.2018	Final check and submission	Mikko Pihlatie	VTT



Executive Summary

This report is the status of the considered electrical motor technology, design approaches, evaluation matrix and concept decision for the proposed modular drive train system [1] of the DRIVEMODE project at his released date.

The electrical motor technologies and design approaches are all the time evolving as well as this document. WP3 will update this document constantly with new scientific research achievements and activities, new technological recognitions, boundary information and decisions as soon as they arise, defined and agreed by the DRIVEMODE consortium.

First section of the report defines the background, purpose and use of the document.

The second section presents the scientific literature overview, technological demands, E-machine topologies overview and specifies the functional requirements of the electrical machine. The third section presents and defines the main E-machine components, their design aspects and considered electric motor technologies.

The fourth section presents calculation methodologies as a multi-physical approach to the design and to optimization of E-machine.

The fifth section shows the E-machines concept result.

The sixth section presents the evaluation matrix and the evaluation results.

The seventh section gives the concept decision and further focus in development of E-machine

The final section declares the evaluated approaches have been presented and that all new achievements will be presented in the upcoming reports.

Attainment of the objectives and if applicable, explanation of deviations

The report on considered electrical motor technologies, evaluation matrix and concept decision contains all data available at the date of delivery 31. July. It gives a detailed benchmark overview of E-machines applied in electric vehicles and industrial applications through the literature overview. The basic e-machine components and the approaches for their design as well as, the possible problems and drawbacks during the design and development are presented in detail. These lead to the definition and further on applied electrical motor technologies during the work in Task 3.1 and Task 3.2. Based on the considered e-motor technologies the two concept designs are involved, they are; the Permanent Magnet Synchronous Machine (PMSM) and the Induction Machine (IM). The evaluation matrix based on multi-attribute utility theory and derivatives method for decision-making leads to the electric motor concept decision, which is PMSM. It can be clearly stated that all deliverable related task objectives were achieved. The selected e-motor concept is used and will be used in all upcoming Tasks (T3.2, T3.3, T3.4, T3.5 and T3.6) in WP3.

The deliverable has been delayed by two months to include all the latest material available on electrical motor design from various partners. The delay has not affected the project or parties in it as it summarises the information that is internally available.



Table of contents

D3.2: Report on considered electrical motor technologies, evaluation matrix, concept decision WP 3, T 3.1 and T 3.2	1
Author: Damijan Miljavec (UL)	1
Technical references	2
Executive Summary	4
Attainment of the objectives and if applicable, explanation of deviations	4
Table of contents	5
List of Tables	6
List of Figures	6
1. Purpose	8
1.1. Introduction DRIVEMODE	8
1.2. Scope of document	8
1.3. Compliance with Specification	8
2. E-Machine functional requirements and Literature overview	9
2.1. General functional requirements of traction E-Motor	9
Development Basis and Choice of technology	9
2.2. Scientific literature overview of electric vehicle (EV) traction E-machines	11
E-Machine [6]-[8]	14
E-machine [9]-[11]	15
E-machine [12]	17
E-Machine [24]	19
2.3. Summary	21
3. Considered electric motor technologies	22
3.1. Traction E-machine components general classification	22
3.2. Stator	22
3.3. Stator windings	24
3.4. Rotor	28
3.5. Air-gap	30
3.6. Shaft	30
3.7. Stator housing	31
3.8. E-machine control	31
3.9. Rotor skewing	32
3.10. Parasitic effects	32
4. Calculation Methodology	36
4.1. Electromagnetic analyses	36
4.2. Thermal analyses	36
4.3. Mechanical analyses	36



5. Concepts results	38
5.1. PMSM V2a results.....	38
5.2. IM V5a results	44
6. Evaluation matrix	49
7. Concept decision.....	51
8. Conclusions	52
9. References	53
10. Appendices	54
10.1. List of abbreviations	54

List of Tables

Table A Electric machine benchmark results	11
Table B Toyota Prius 3rd generation electric machine properties	14
Table C BMW i3 electric machine properties	15
Table D Nissan Leaf electric machine properties	17
Table E AUDI APA250 electric machine properties.....	19
Table F Electromechanical performance at peak operational conditions for PMSM V2a	38
Table G Mechanical properties of PMSM V2a	38
Table H Masses of different PMSM V2a machine parts and total mass	39
Table I Properties of applied permanent magnets	40
Table J Working points for PMSM performance evaluation	42
Table K Characteristic operation points IM of IM V5a	44
Table L Dimensions of IM V5a	45
Table M Weight of IM V5a	46
Table N Working points for IM V5a performance evaluation	46
Table O Weighted Decision Matrix -DriveMode Concepts.....	49
Table P Comparison between different automotive main electrical machine	50

List of Figures

Figure 1 Peak and continuous torque specification of E-Motor	10
Figure 2 Peak and continuous power specification of E-Motor	11
Figure 3 Toyota Prius 3rd generation electric machine cross section (E-Machine [6]-[8]).....	15
Figure 4 BMW i-3 machine stator cross section (E-machine [9]-[11])	16
Figure 5 BMW i-3 machine rotor cross section (E-machine [9]-[11]E-machine [9]-[11]) ...	17
Figure 6 Efficiency map for BMW-i3 electric machine (E-machine [9]-[11])	17
Figure 7 Nissan Leaf electric machine stator and rotor cross section (E-machine [12])	18



Figure 8 Efficiency map for the Nissan Leaf electric machine (E-machine [12]).....	19
Figure 9 AUDI APA250 electric machine stator	20
Figure 10 AUDI APA250 electric machine rotor.....	20
Figure 11 AUDI APA250 electric machine performance	21
Figure 12 Slot leakage magnetic flux density	22
Figure 13 Magnetic flux concentration and distribution across stator teeth.....	23
Figure 14 B-H curve of NO20.....	24
Figure 15 Interpolated specific iron losses for NO20 based on measured points.....	24
Figure 16 Fundamental winding factors.....	25
Figure 17 Winding harmonic components for 36 slots and 8 poles.....	25
Figure 18 Winding harmonic components for 27 slots and 8 poles [25]	26
Figure 19 Concentrated winding layout for 12 slots and 10 poles, a: single layer, b: double layer [25].....	27
Figure 20 Distributed winding layout for 36 slots and 8 poles [25]	27
Figure 21 Distributed winding layout for 27 slots and 8 poles [25]	27
Figure 22 Temperature dependent B-H curve of PM type BMN-42UH/ST	29
Figure 23 Magnetic flux density normal component B_z (in z-direction, along the machine axis) distribution at no-load conditions almost (0.1 mm above) on the stator end-sheet surface	33
Figure 24 Magnetic flux density normal component B_z (in z-direction, along the machine axis) distribution at no-load conditions almost (0.1 mm above) on the stator end-sheet surface	33
Figure 25 Magnetic flux density normal component B_z (in z-direction, along the machine axis) distribution at no-load conditions almost (0.1 mm above) on the stator end-sheet surface	34
Figure 26 Magnetic flux density normal component B_z (in z-direction, along the machine axis) distribution at load conditions almost (0.1 mm above) on the stator end-sheet surface	35
Figure 27 Magnetic flux density normal component B_z (in z-direction, along the machine axis) distribution at load conditions almost (0.1 mm above) on the stator end-sheet surface	35
Figure 28 Peak torque speed curve for PMSM V2a.....	40
Figure 29 Peak power versus speed curve for PMSM V2a.....	41
Figure 30 Efficiency curve for peak operational points at 130 °C.....	41
Figure 31 Efficiency map of PMSM V2a.....	42
Figure 32 PMSM V2a cross section for thermal study	43
Figure 33 Temperature rise in different machine part during continuous operational mode ...	43
Figure 34 Temperature rise in different machine part during peak power operational mode for 60 seconds at ambient temperature 100 °C	44
Figure 35 Torque speed-characteristics of designed and evaluated induction machine Var5a .	45
Figure 36 IM V5a cross section for thermal study.....	47
Figure 37 IM V5a: Temperature rise in different machine part during continuous operational mode.....	47
Figure 38 IM V5a: Temperature rise in different machine part during continuous operational mode at maximum speed	48
Figure 39 IM V5a Temperature rise in different machine part during peak power operational mode for 60 seconds at ambient temperature 100°C	48



1. Purpose

1.1. Introduction DRIVEMODE

DRIVEMODE is a project funded by the European Commission under the Horizon 2020 framework. The project aims at designing a compact modular integrated drive module (IDM) for pure electric vehicles (PEVs) and hybrid electric vehicles (HEVs).

The IDM developed in the DRIVEMODE project will be a drivetrain platform that then can be adopted depending on the application e.g. demonstration vehicle. The modularity and scalability of the IDM will be used to cater to a wider range of application. This document will specify the requirements on component level for the electrical motor including the extent of scalability and modularity expected from the IDM that needs to be fulfilled to meet the project objectives

1.2. Scope of document

This report is the status of the considered electrical motor technology, design approaches, evaluation matrix and concept decision for the proposed modular drive train system of the DRIVEMODE project at his released date. The E-Motor's active parts shall be described, evaluated, designed, calculated and optimized in the design stage. In the prototype manufacturing stage, the motor shall be inserted into housing and coupled to an inverter and transmission to form an integrated drive module (IDM).

1.3. Compliance with Specification

Discrepancies or deviations within this specification are to be indicated without delay by the WP3. Possible solutions have to be discussed with DRIVEMODE partners.



2. E-Machine functional requirements and Literature overview

2.1. General functional requirements of traction E-Motor

The functional requirements used and briefly presented in this report are based on statements presented in deliverable D3.1 report [2] (Wand 2018). They are serving as basis and boundaries in research, design, analysis and development of E-machines presented in details in this deliverable D3.2 report.

Development Basis and Choice of technology

Within the DRIVEMODE project the WP3 evaluated two E-Machine technologies in detail:

- Permanent magnet synchronous machine (PMSM)
- Induction motor (IM), squirrel cage asynchronous motor

The E-machine development bases presented in D3.1 [2] (Wand 2018) are summarized in the following text.

- For traction E-Motors with the wide speed range capability and the high efficiency aspects many representative load points have to be simultaneously investigated. The best efficiency contour of the torque speed characteristic should coincide with its most frequent operating points.
- Material
Improved steel grades and thinner laminations shall be used
- Windings
Proper winding configuration and technology shall be selected.
Windings and winding material shall sustain problems with high switching frequencies and high dV/dt due to new SiC switch technology
- Driving aspects
Increased iron and copper losses due to high rotational speeds and high driving frequencies shall be considered.
Sinusoidal space vector pulse width modulation (SVPWM) will be used to drive E-Machine and applying field oriented control (FOC) with implemented maximum torque per ampere (MTPA) motor control algorithm.
- Mechanical aspects
Designed high speed E-Machine shall sustain high mechanical stresses. And, used materials must withstand the height mechanical forces and vibrations.
- Thermal aspects
Improved cooling shall be achieved to increase the E-Machine over-load-ability and to avoid permanent magnets demagnetization.



The E-machine should fulfil the performance requirements shown in Figure 1 **Error! Reference source not found.** and Figure 2 **Error! Reference source not found.**. They are taken out from the Preliminary system specification and from D3.1 report [2] (Wand 2018) directly.

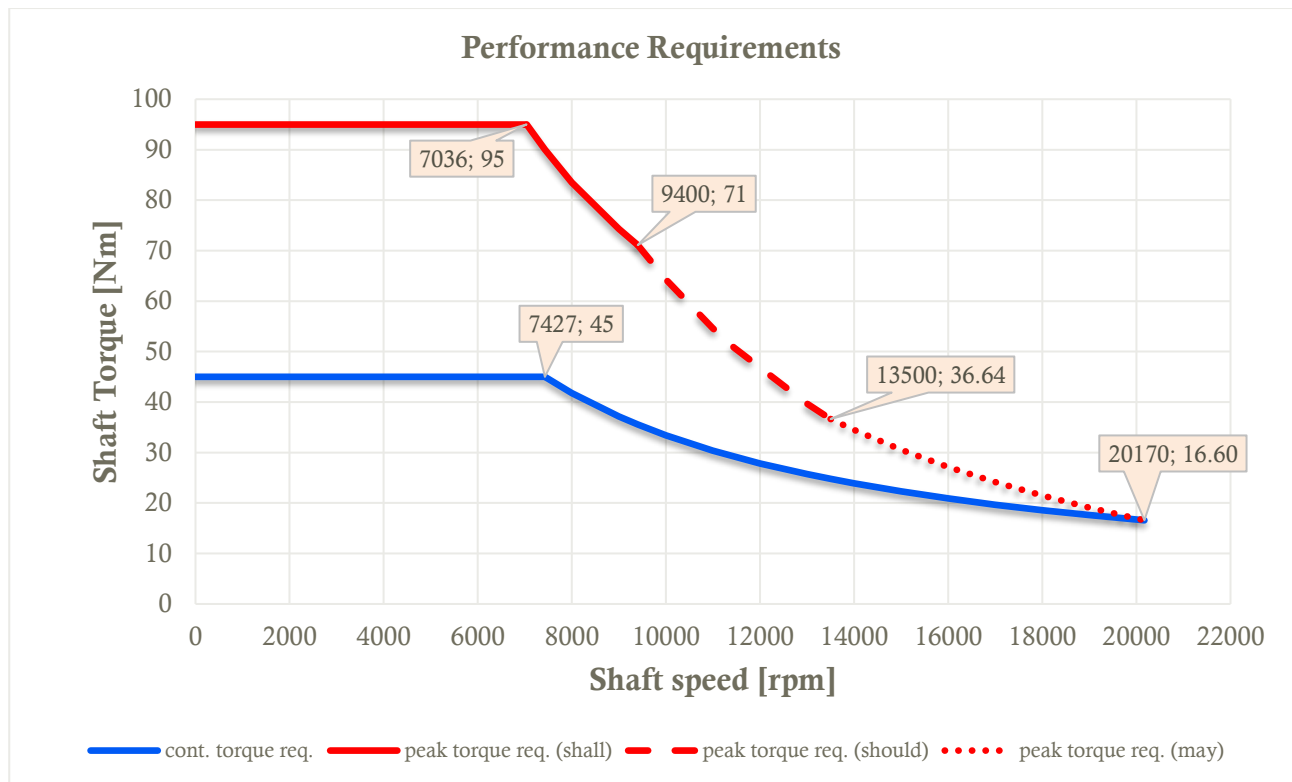


Figure 1 Peak and continuous torque specification of E-Motor



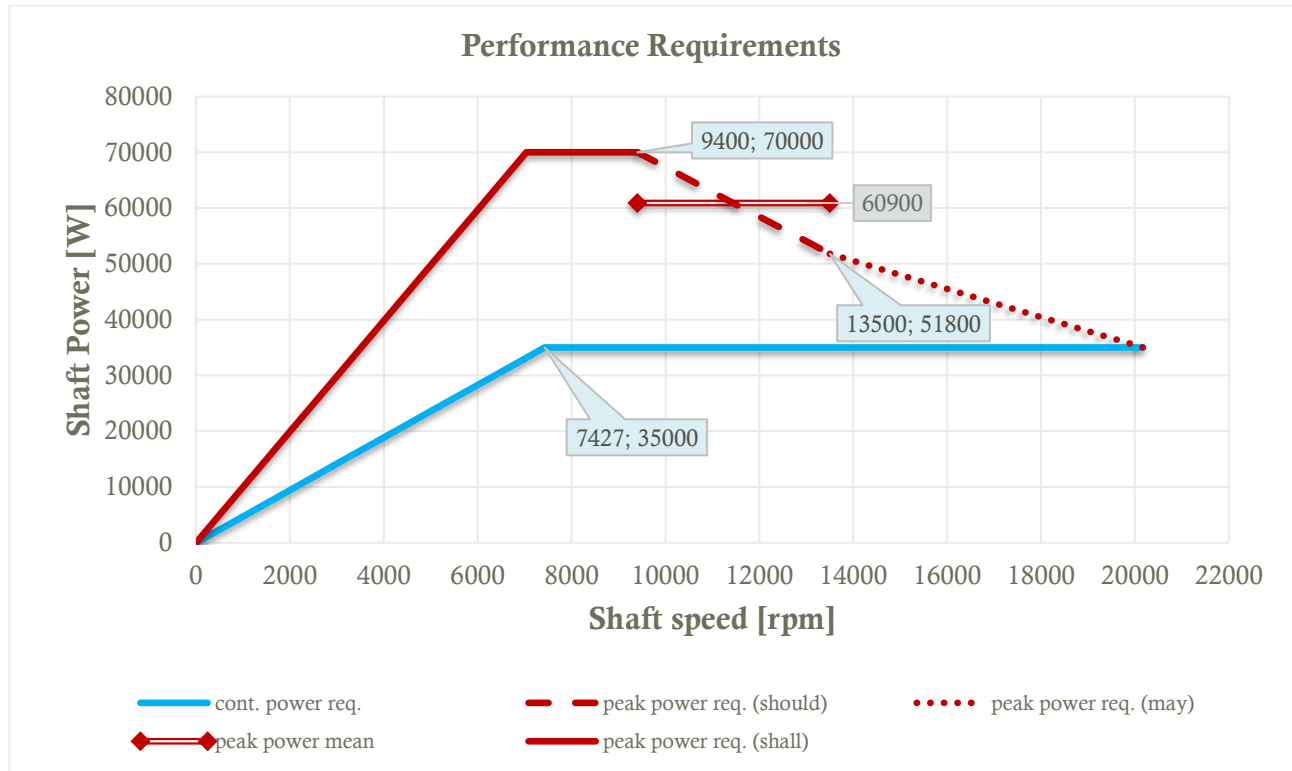


Figure 2 Peak and continuous power specification of E-Motor

2.2. Scientific literature overview of electric vehicle (EV) traction E-machines

During the preliminary development as well as in the design phase the scientific literature was studied and used in the design of DRIVEMODE e-machines. The patents were analysed to avoid IP conflicts. The solutions known from scientific literature were applied to the design process. The project researcher's previous knowledge were also used during the design, analyses, optimisation and verification phases. The benchmark was also done during the research work. The main benchmark results are presented in Table A and further in the text.

Table A Electric machine benchmark results

Machine	P (kW)	U _{dc} (V)	Reference/Source	Notes
[3]	150	720	Pia Lindh (Juha Pyrhönen): Multidisciplinary design of a permanent-magnet traction motor for a hybrid bus taking the load cycle into account, 2016	Juha Pyrhönen's paper about the electric motor for a bus.
[4]	10	120	Liang Chen: Reduced dysprosium permanent magnets and their applications in electric vehicle traction motors, 2015	Paper focusing mainly on magnet material, so some information is missing.



Machine	P (kW)	U _{dc} (V)	Reference/Source	Notes
[5]	30	325	Ayman M. EL-Refaie: Advanced high-power-density interior permanent magnet motor for traction applications, 2014	Concentrated winding was used in the paper, but DES returns 2-L distributed by default, and with manual settings 1-L distributed is used (efficiency with concentrated is too low).
[6]	60	650	Kyohei Kiyota: Comparison of test result and design stage prediction of switched reluctance motor competitive with 60 kW rare-earth PM motor, 2014	Toyota Prius 3rd generation motor
[7]			Kyohei Kiyota: Design of switched reluctance motor competitive to 60 kW IPMSM in third generation hybrid electric vehicle, 2011	
[8]			James R. Hendershot: MotorSolve analysis of the 2010 Toyota Prius traction motor, 2015	
[9]	125	380	J. Merwerth: The hybrid-synchronous machine of the new BMW i3 and i8, 2014	BMW i3 motor
[10]			Tim Burress: Benchmarking EV and HEV technologies, 2016	
[11]			David Staton: Open source electric motor models for commercial EV and hybrid traction motors, 2017	
[12]	80	360	Tim Burress: Benchmarking state-of-the-art technologies, 2013	Nissan Leaf
[11]			David Staton: Open source electric motor models for commercial EV and hybrid traction motors, 2017	
[10]	124	700	Tim Burress: Benchmarking EV and HEV technologies, 2016	Honda Accord
[13]			Honda Accord Model Information, http://owners.honda.com/vehicles/information/2014/Accord-Hybrid/specs#mid^CR6F3EEW , 2018	



Machine	P (kW)	U _{dc} (V)	Reference/Source	Notes
[8]	165	288	James R. Hendershot: MotorSolve analysis of the 2010 Toyota Prius traction motor, 2015	2008 LS 600 h
[14]			Mitch Olszewski: Evaluation of the 2008 Lexus LS 600H hybrid synergy drive system, 2009	
[8]	105	245	James R. Hendershot: MotorSolve analysis of the 2010 Toyota Prius traction motor, 2015 Mitch Olszewski: Evaluation of the 2007 Toyota Camry hybrid synergy drive system, 2008	Hybrid Camry
[16]	160	650	Siemens catalogue of several different motors	Siemens PEM-Motor 1DB2016 – WS54
[16]	200	650	Siemens catalogue of several different motors	Siemens PEM-Motor 1DB2022 – WS36
[16]	320	750	Siemens catalogue of several different motors	Siemens PEM-Motor 1DB2024 – WS36
[17]	30	516	Jingjuan Du: Optimization of magnet shape based on efficiency map of IPMSM	IPM-V-I rotor used in the paper
[18]	2,6	42	Jin Hur: Characteristic analysis of IPM synchronous motor in electrohydraulic power steering systems, 2008	Small motor
[19]	5	120	Jiabin Wang: Design optimization of a surface-mounted permanent-magnet motor with concentrated windings for electric vehicle applications, 2013	/
[20]	1,4	42	Tao Sun: Effect of pole and slot combination on noise and vibration in permanent magnet synchronous motor, 2011	/
[21]	110	750	You-Young Choe: Comparison of concentrated and distributed winding in an IPMSM for vehicle traction, 2012	/



Machine	P (kW)	U _{dc} (V)	Reference/Source	Notes
[22]	79	650	Parker catalogue: Electric and hybrid vehicle - Accessory, power generation and traction motor solutions, 2014	One of the Parkers' motors from the catalogue
[23]			Parker catalogue: GVM Global Vehicle Motor, 2017	
[24]	135	360	Wiener Motoren Symposium 2018, Audi AG, S. Pint, N. Ardey, G. Mendl, G. Fröhlich, R. Straßer, T. Laudenbach, J. Doerr	AUDI APA250

Machines studied, analysed and presented in Table 1 are applicable to different industry branches. For us the most important e-machines are that one applied to electric and hybrid vehicles. Further on, the e-machines [6]-[8], [9]-[11] and [12] (Table A) applied in automotive vehicles are presented in more details.

E-Machine [6]-[8]

The machine under the references [6]-[8] is the Toyota Prius 3rd generation electric machine. The performance characteristics are shown in Table B.

Table B Toyota Prius 3rd generation electric machine properties

	Original data	
U _{DC} (V)	650	DC voltage
T _m (Nm)	100 -> estimated from (27 kW battery power)/(60 kW peak power)*(207 Nm)	Nominal torque
n ₀ (rpm)	2768	Base speed
n _m (rpm)	13900	Maximum speed
magnet type	NdFeB	
winding type	N/A	
rotor type	IPM-V	V shape PM distribution
cooling type	Indirect liquid	
p	4	No. Pole pairs
q	2	Pole per slot per phase



	Original data	
z_s	11	No. turns per coil
δ (mm)	0,73	Air gap
h_{mag} (mm)	7,16	Magnet height
l_{mag} (mm)	17,9	Magnet length
d_{se} (mm)	264	Stator outer diameter
d_s (mm)	161,9	Stator inner diameter
d_r (mm)	160,4	Rotor outer diameter
l (mm)	50	Stator/rotor length

The machine cross section is shown in **Error! Reference source not found..**

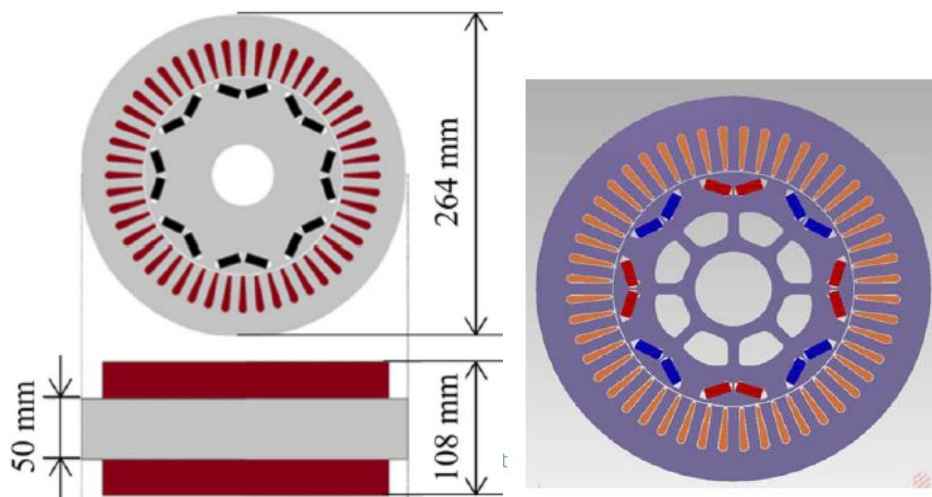


Figure 3 Toyota Prius 3rd generation electric machine cross section (E-Machine [6]-[8])

E-machine [9]-[11]

The machine under the references [9]-[11] is the BMW i3 electric machine. The performance characteristics are shown in Table C.

Table C BMW i3 electric machine properties

	Original data
U_{DC} (V)	380
T_m (Nm)	250



	Original data
n ₀ (rpm)	4500
n _m (rpm)	11400
magnet type	NdFeB
winding type	assumed 1-L distributed
rotor type	IPM-I
cooling type	Indirect liquid
p	6 pole pairs
q	2 slots/pole/phase
z _s	N/A
delta (mm)	N/A
h _{mag} (mm)	N/A
l _{mag} (mm)	N/A
d _{se} (mm)	N/A
d _s (mm)	N/A
d _r (mm)	N/A
l (mm)	N/A

The BMW i-3 machine stator cross section is shown in Figure 4 and rotor in Figure 5. The mass of the machine without the shaft is 50kg. Efficiency map is given in Figure 6.

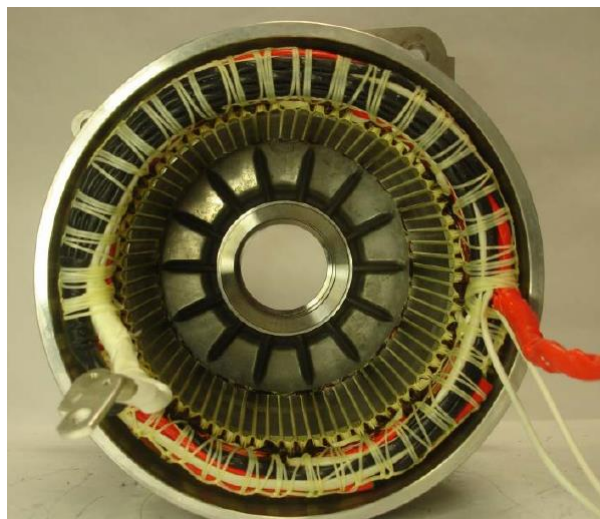


Figure 4 BMW i-3 machine stator cross section (E-machine [9]-[11])



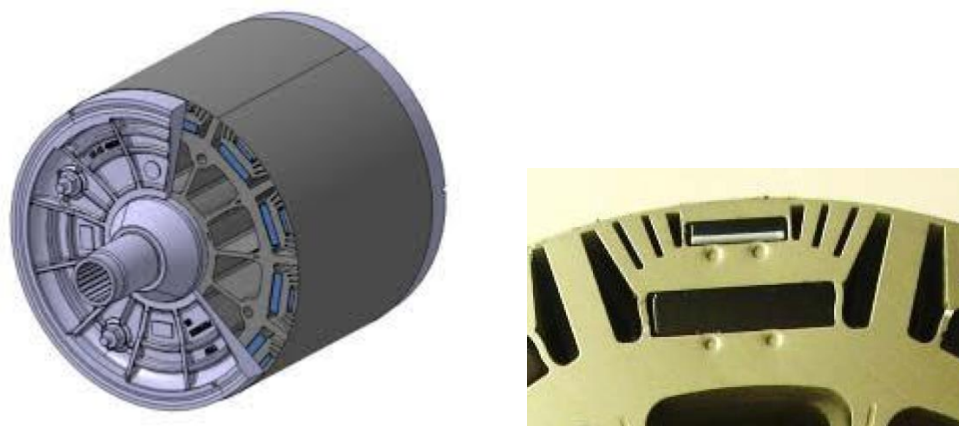


Figure 5 BMW i-3 machine rotor cross section (E-machine [9]-[11])

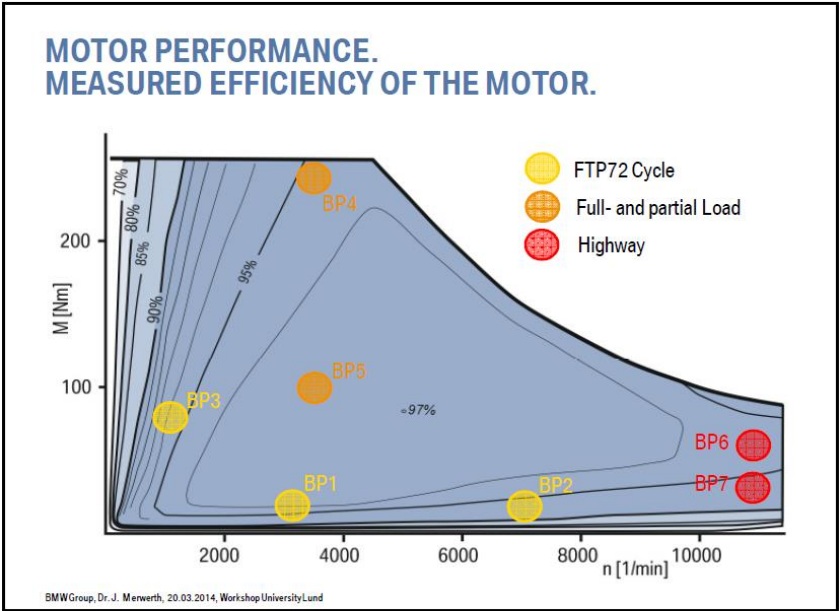


Figure 6 Efficiency map for BMW-i3 electric machine (E-machine [9]-[11])

E-machine [12]

The machine under the reference [12] is the Nissan Leaf electric machine. The performance characteristics are shown in Table D.

Table D Nissan Leaf electric machine properties

	Original data
U _{DC} (V)	360
T _m (Nm)	280
n ₀ (rpm)	2728

	Original data
n_m (rpm)	10390
magnet type	N/A (assumed NdFeB)
winding type	assumed 1-L distributed
rotor type	IPM-VI
cooling type	Indirect liquid
p	4 pole pairs
q	2 slots/pole/phase
z_s	20
delta (mm)	0,5, air-gap
h_mag (mm)	N/A
l_mag (mm)	N/A
d_se (mm)	198,12 (stator outer diam.)
d_s (mm)	130,96 (stator inner diam.)
d_r (mm)	129,97 (rotor outer diam.)
l (mm)	151,16 (stator/rotor length)

The Nissan Leaf electric machine stator and rotor cross section are shown and rotor in Figure 7 **Error! Reference source not found..**

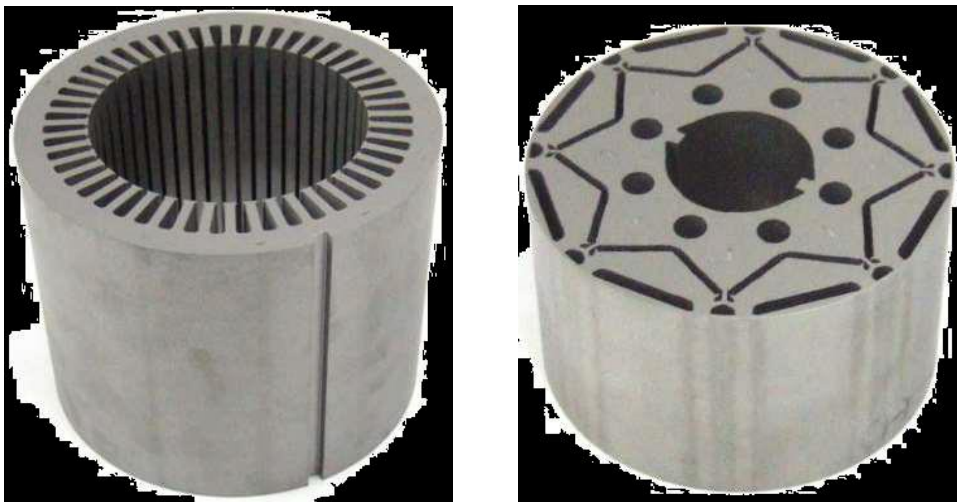


Figure 7 Nissan Leaf electric machine stator and rotor cross section (E-machine [12])



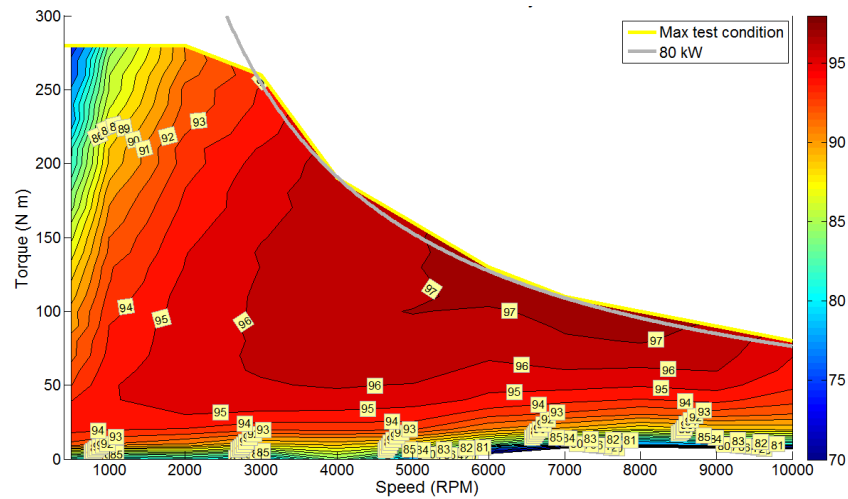


Figure 8 Efficiency map for the Nissan Leaf electric machine (E-machine [12])

E-Machine [24]

The machine under the reference [24] is the AUDI APA250 electric machine. The electric machine properties are shown in Table E.

Table E AUDI APA250 electric machine properties

	Original data
U_DC (V)	360
T_m (Nm)	247
Current, cont. (A)	240
n_max (rpm)	15000
Peak power (kW)	125
winding type	distributed
rotor type	A1 (99.7% pure) squirrel cage
cooling type	Indirect liquid, stator water jacket, rotor shaft water cooling
Stator /rotor slots	48 / 56
p	2 pole pairs
d_s (mm)	245
Air gap (mm)	0.6



	Original data
d _r (mm)	156
l (mm)	120

The AUDI APA250 electric machine stator and rotor are shown and rotor in Figure 9 and Figure 10.

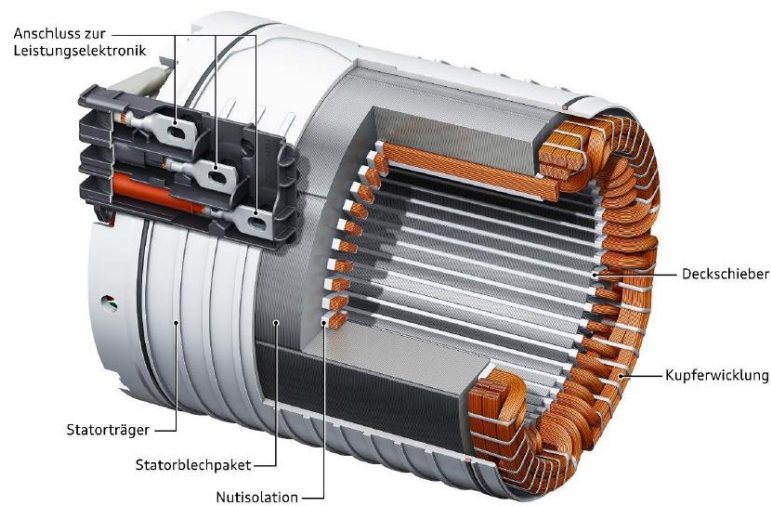


Figure 9 AUDI APA250 electric machine stator

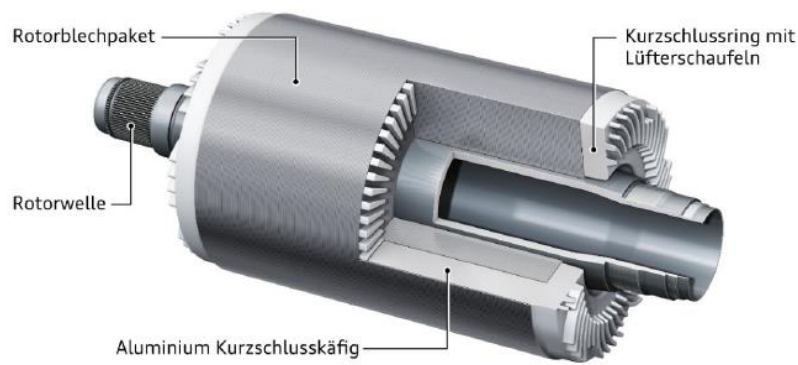


Figure 10 AUDI APA250 electric machine rotor

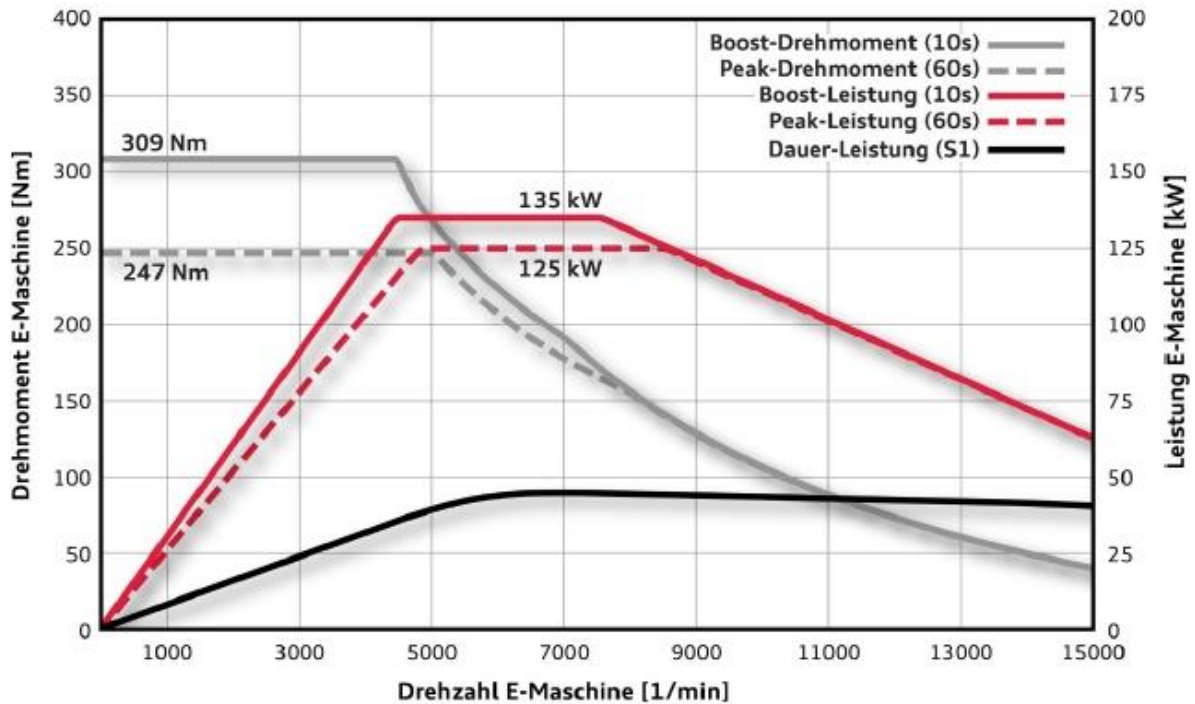


Figure 11 AUDI APA250 electric machine performance

2.3. Summary

Starting from this study the IPM (Interior Permanent Magnet synchronous machine) and the IM (Induction Machine) were selected as the main e-motor technologies for the DRIVEMODE IDM. Both technologies are mature and SOP (start of production) ready for series production by the year 2020.

The realized e-motors in the study use fluid cooling for high performance, as will DRIVEMODE. Due to the constraints of the cooling circuit available in the demonstrator vehicle, only outer fluid cooling with water/glycol is possible. Advanced direct cooling of the stator winding or cooling of the rotor as in the AUDI is not possible. This would be preferable for performance but contradicts the low cost target and modularity objective of the DRIVEMODE project.

The speed range is up to 16.000 rpm. So the DRIVEMODE e-motor will investigate the benefits and challenges of the higher speeds up to ~22.000 rpm. This maximum speed is the result of the selected transmission ratio and vehicle performance requirements.

The winding technology will be round wire windings. Hairpin technology has better copper fill factor and therefore lower losses in the winding, but the initial for cost the production design is exceptional higher than for round wire windings, so WP3 aimed for the later to implement in the demonstrator.



3. Considered electric motor technologies

3.1. Traction E-machine components general classification

The components of E-machine are stator, rotor, permanent magnet, winding, housing and shaft. These components are presented in details, studied, dimensioned, designed, analysed and optimized. Accordingly to previously described basis of development and choice of technology the main components are evaluated.

3.2. Stator

- Inner diameter
Inner diameter is defined accordingly by the rotor outer diameter and air-gap thickness.
- Outer diameter
Stator outer diameter is defined by overall available dimensions and depend on the housing geometric and cooling properties of the housing. The value is also defined by stator slot area, stator yoke thickness, number of slots, slot insulation thickness, slot leakage magnetic flux density and winding technology
- Number of slots
Their number is defined by the by the winding type, winding technology, winding configuration and number of magnetic poles.
- Number of poles
The number is defined by rotational speed, stator magnetic loadings, end-windings and inverter maximum fundamental driving frequency
- Number of phases
The number is defined by inverter topology, amount of energy transferred to the E-Machine, level of torque pulsation, safety issue and power supply redundancy.
- Stator slot design
The design depends on slot leakage magnetic flux density (Figure 12), winding fill factor, slot insulation thickness, winding arrangements, and winding technology.

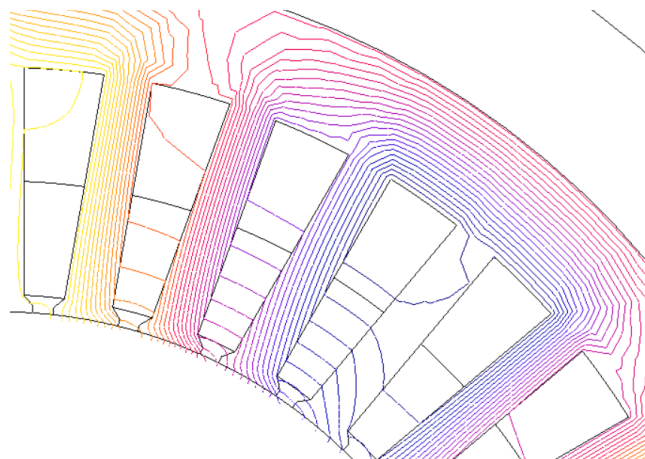


Figure 12 Slot leakage magnetic flux density



DRIVEMODE stator selected technologies/solutions have been: diameter and length smaller than WP1 and WP2 defined space limitations, slot number in accordance to pole pair and winding factors that is 36 slots and 8 poles, the topology of frequency inverter defined the number of phases – 3 phases.

- Stator teeth design

Stator teeth design depends on teeth shoe (tip) shape which acts on magnetic flux concentration (Figure 13) and on teeth shoe shape leakage flux. Also the slot opening co-ordinates the level of cogging torque and torque pulsations.

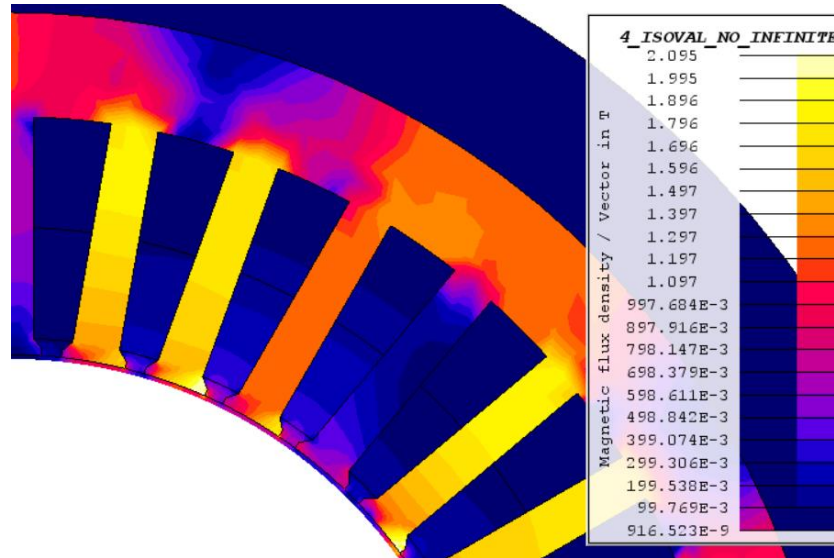


Figure 13 Magnetic flux concentration and distribution across stator teeth

DRIVEMODE stator teeth design selected technologies/solutions have been: saturation level defined the teeth thickness and acceptable flux leakage level defined the height of teeth.

- Stator ferromagnetic material

Stator material usage is defined by the level of magnetic load-ability and applied rotating magnetic flux density (dependent on number of poles and rotational speed). The high quality electrical steel shall be used as stator material (Figure 14). The material properties must be: high permeability on wide excitation range, very thin to reduce eddy currents, high quality to reduce hysteresis losses. Interpolated specific iron losses for electrical steel sheet NO20 based on measured points are shown in Figure 15, as an example. The stator lamination electrical steel sheet manufacturing process should be punching. The laser cutting technology may (will) bring additional parasitic effects as reduction of permeability and increase of iron magnetic losses.



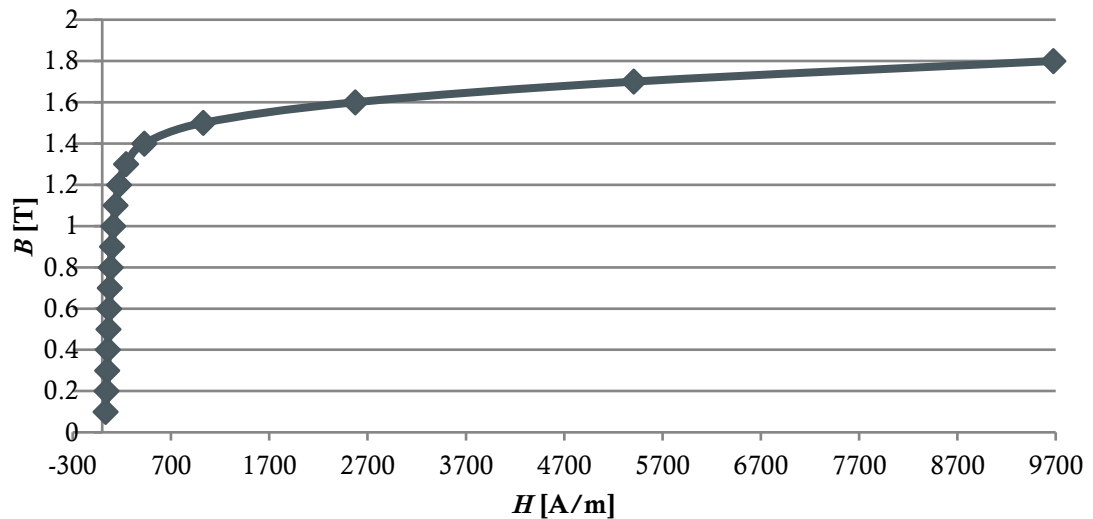


Figure 14 B-H curve of NO20

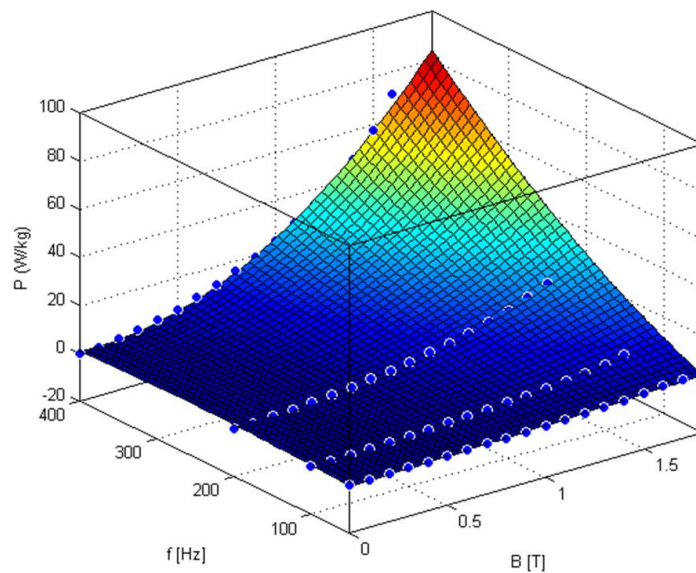


Figure 15 Interpolated specific iron losses for NO20 based on measured points

DRIVEMODE stator ferromagnetic material selected technologies/solutions have been: the losses must be as low as possible due to high driving frequencies and the mechanical strength must be high enough to withstand high speeds, the used material in NO20-1200.

3.3. Stator windings

- Number of slots per pole per phase
The value depends on available space, winding type and pole pairs. This is one of the first decision making parameter.
- Winding factor



Through this value the winding and copper utilization is defined. The tendency is to have the value of winding factor as close to one (Figure 16). It represents the space sum of induced voltage in all space shifted coils placed in the stator slots.

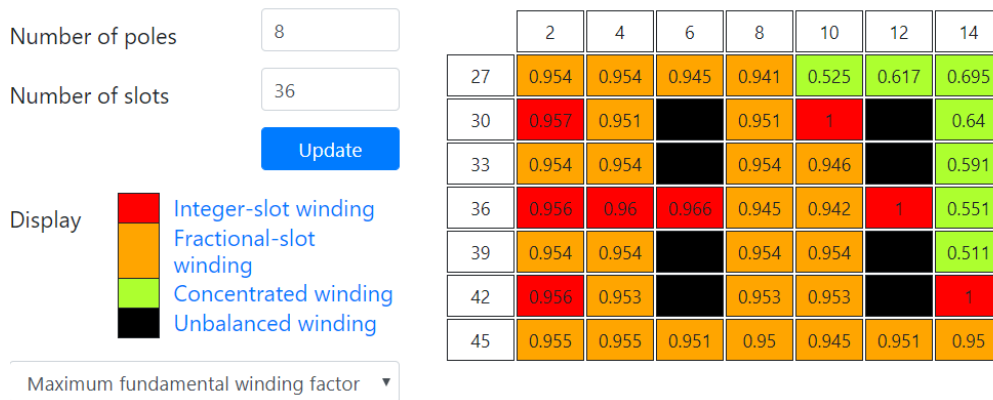


Figure 16 Fundamental winding factors

- Winding harmonic components

The goal is to have just basic harmonic component without high harmonics. But, due to stator slot discretization there will always present undesirable harmonics. In Figure 16 and Figure 17 are presented two different winding arrangements with different high harmonic content. Basically it is convenient to have low level of 5th, 7th, 11th, 13th, ... , $(6k \pm 1)$, where k is an integer. In Figure 17 we can see high level of winding sub-harmonic components which can cause eccentric magnetic rotor pull.

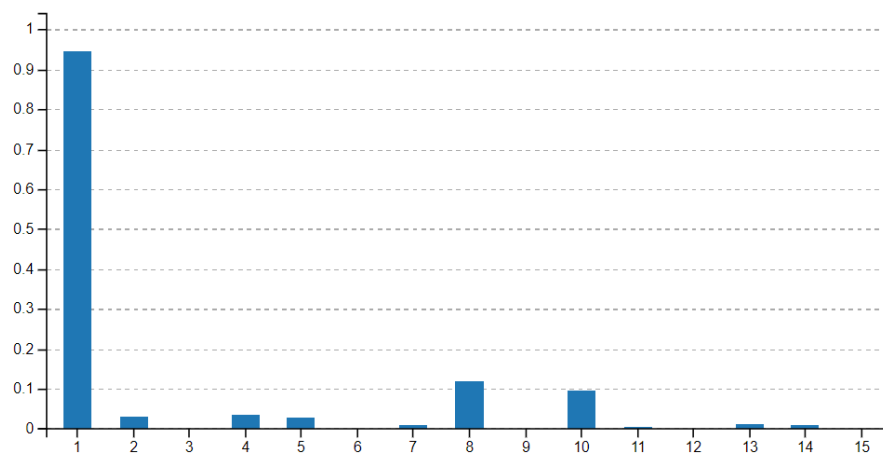


Figure 17 Winding harmonic components for 36 slots and 8 poles



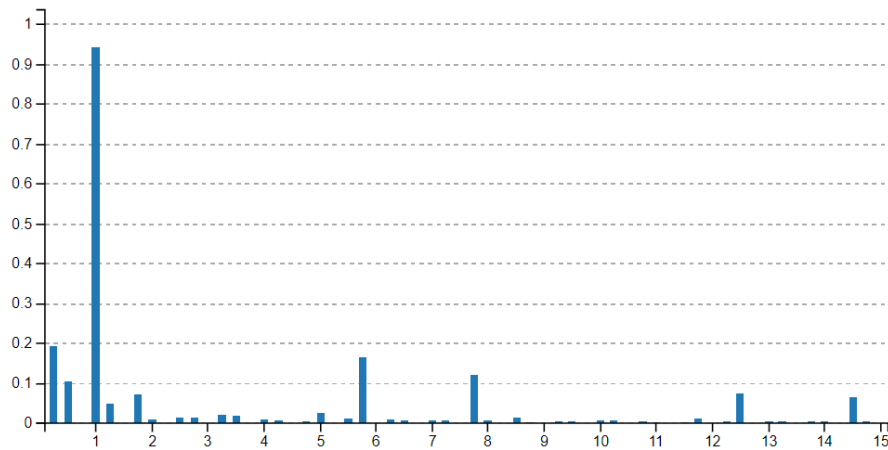


Figure 18 Winding harmonic components for 27 slots and 8 poles [25]

- Copper fill factor

The value should be close to one. But, due to available winding forming technology using classic strained coils the achievable copper fill factor is in the range from 0.4 to 0.45. By applying novel hair pin winding technology the achievable copper fill factor is in the range from 0.6 to 0.7.

- Copper wire

The copper wire is classically with circular cross section with double varnish layer as electrical insulation. Using the hair pin technology winding wire is in rectangular form, with this higher fill factor is achieved. But, the stator slot cross section must be redesigned to the parallel slot edges. Meanwhile, the stator teeth become somehow conical.

The copper wire, which forms the coil, inserted in to the slot has to be properly chosen to counteract the increased copper losses due to high current frequencies (skin effect) and slot magnetic flux leakage. The strained coil conductor form shall be used.

- Type of windings

Generally, there are two types of windings. First type of windings is concentrated windings (Fig. 18), where the coils are wound around each tooth or around every second tooth. These windings are easy to wound and the length of end-winding is short. The problem is in the content of high harmonic components and in the content of high harmonics in the air-gap magnetic flux density due to reluctance variation and due to stator current ripple pulse width modulation (PWM). The effect of both phenomena is in flux pulsations in rotor structure which leads to additional rotor iron losses and permanent magnet eddy current losses. This type of windings is not suitable for induction machine, just for permanent magnet machines. The second type of winding is distributed winding (Figs. 19. and 20), where the coils are wound around every third or fourth or n^{th} tooth. They can have a form of short pitched winding to reduce winding higher harmonics. Applying this type of winding the magnetic flux density in the air gap has more sinusoidal shape and there is almost no influence on constant magnetic flux density in rotor structure. The main drawback of this winding type is the larger end-windings. These large end-windings can be reduced by applying higher number of pole pairs, but with higher rotational speeds this leads to higher driving frequencies with increased iron and copper losses.



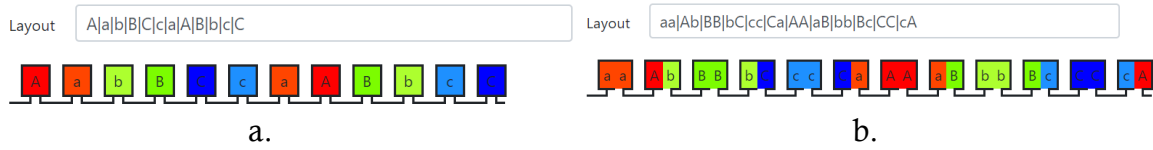


Figure 19 Concentrated winding layout for 12 slots and 10 poles, a: single layer, b: double layer [25]

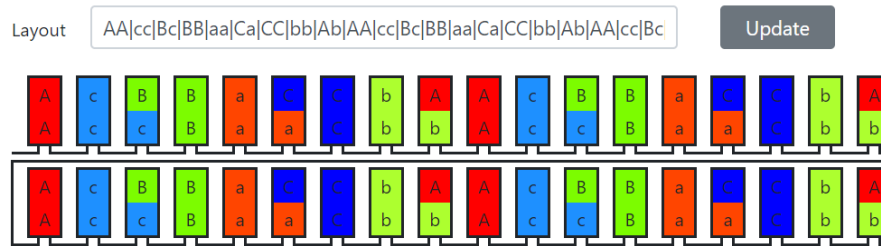


Figure 20 Distributed winding layout for 36 slots and 8 poles [25]

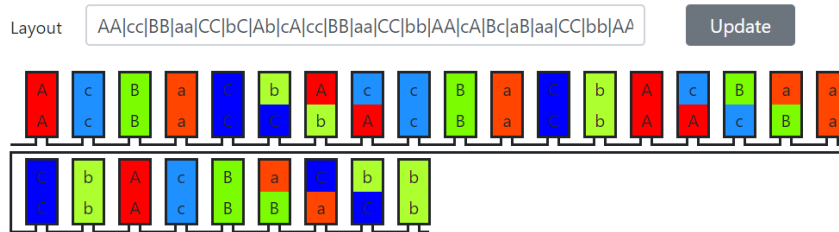


Figure 21 Distributed winding layout for 27 slots and 8 poles [25]

- Winding technology

The hair-pin winding technology has many advantages over classical stranded coil winding technology. We can achieve better thermal conductivity of the slot (copper losses in form of excessive heat is better transferred to the stator iron sheet) and better copper fill factor. On the other hand we have to pay attention on stator slot magnetic flux leakage and further on additional high harmonic copper losses. This is even more evident in high speed e-machine drive configuration. The copper welding (laser, electrical) process must be controlled when using hair-pin winding technology.

DRIVEMODE stator windings selected technologies/solutions have been: regarding the available space the “Number of slots per pole per phase” is 1.5, the Winding factor of 0.945 to increase as high as possible the winding utilisation, Winding harmonic components - lower numbers of harmonic with the lowest possible value, Copper fill factor highest as possible to better utilize copper wire and slot cross section $K_{cu}=0.413$, Copper wire which forms the turn/coil/winding is stranded and one wire depends on skin effect and leakage flux effect – the diameter lower than 0.8 mm, the Type of windings is distributed with the goal to move closer to the sinusoidal shape of induced voltage, the classic available Winding technology shall be used.



DRIVEMODE stator thermal aspect selected technologies/solutions have been: accordingly to the chosen copper wire insulation grade (defined by varnish temperature class) the stator temperature must be kept in the range below 160 °C.

3.4. Rotor

The rotors are completely different for induction machine and permanent magnet machines. Common general facts and some specifics are described below.

- Inner diameter
Rotor inner diameter is defined by shaft diameter.
- Outer diameter
Rotor outer diameter defines the magnetic and electric load-ability and further on torque production. In combination with air-gap length they define the availability of energy conversion in defined volume. The rotor sheet may contain the mass reduction holes. Their shape is specific to applied rotor design.
- Number of poles
The number of poles are defined by chosen number of slots per pole per phase, inverter defined number of phases, stator slot available space and winding type. The maximum operating frequency of the inverter is a limiting factor for high speed machines and the applicable number of poles.
- Number of slots
 - In IM technology the number of rotor slots depends mainly on number of stator slots. Not all combinations are acceptable. We need to pay special attention on this fact. Two type of rotor winding configuration can be applied. First one is made by copper wire coils inserted in rotor slots. The ends are connected to the rotor slip rings. The wound rotor induction machine is formed. This induction machine can be fed from both, rotor and stator, sides. Such design is not suitable for main traction E-machine in automotive application. The wound rotor windings can be replaced with die casted aluminium or copper in rotor slots forming rotor bars and connected with end-rings from both sides. In this way, a so called squirrel cage is formed and it acts as a rotor winding. The torque speed curve shape depends on rotor slot shape and type of used material to form a squirrel cage. The best results are achieved with copper squirrel cage using open rotor slots with semi deep rotor bars.
 - In PMSM technology it is hard to talk about the rotor slots. It is better to say hole/place for permanent magnet insertion. Different positions of PM are available. Their positions in the rotor define the PMSM characteristics. PM can be positioned on rotor surface forming surface rotor PMSM, than, there exist many different rotor types, such as: inset, spoke, consequent pole, buried (I-shape, V – shape, U – shape, UV– shape, UI – shape, UU –shape) and many more.
- Rotor material
Usually, the rotor magnetic material is the same as the stator one. It is economical to use the same material to form stator and rotor with the same length, due to electrical steel scrap reduction.



- Thermal aspect

The rotor temperature must be kept in the range below 120 °C, or more exactly the “safe” temperature depends on the PM grade. The change in rotor (PM) temperature influences the PMSM performance. The PM magnetization level is reduced as the rotor temperature is increased. In the case of IM, increase of rotor temperature increases the squirrel cage resistance and further on this results in torque speed curve slope reduction in the surroundings of nominal working point. On the other side, the IM rotor can sustain higher thermal loadings (higher temperatures) than the PMSM rotor without any damage.

- Demagnetisation

The increase of temperature may cause partial or total demagnetization of the PMs. The worst case happens when the temperature is increased and at the same time high level of d-axis current opposing PM magnetization direction is applied to the stator windings. In this case and with not properly designed rotor this results in partial or total demagnetization of the PMs. The PMs with high remanent magnetization and high coercive magnetic field strength (Fig. 21) are recommended for use in high performance PMSM drive system as in EV.

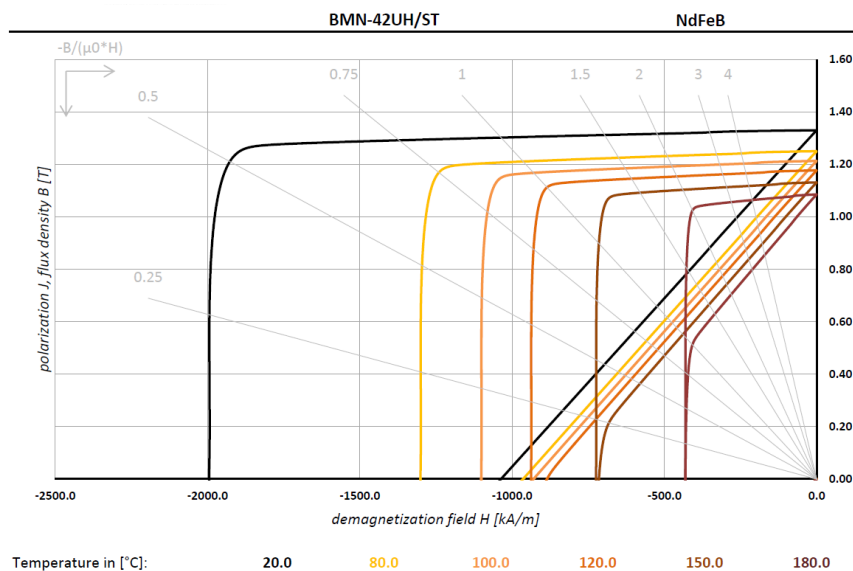


Figure 22 Temperature dependent B-H curve of PM type BMN-42UH/ST
(BOMATEC, www.bomatec.ch)

- Mechanical aspect

The e-machine requirement regarding the rotational speed is posted to the maximum value of 20170 rpm with spinning speed value of 24204 rpm and burst speed of 28238 rpm. This leads to the issue of rotor mechanical strength.

Induction machine with open rotor slots and aluminium bars could have some mechanical problems, due to aluminium property of creeping. Meanwhile, using copper rotor bars this problem is omitted. The special attention must be devoted to the mechanical strength of squirrel cage end-ring connection to the rotor bars (when rotor bars are inserted into rotor slots). In the case when the squirrel cage is made from copper applying die-cast technology this mechanical problem is not problematic.



In the case of PMSM the rotor mechanical strength must be taken even more seriously as in the case of IM. Rotor structure with PM holes must sustain these high speeds. Generally, the rotor sleeve can be used to mechanically strengthen the rotor structure. This leads to the increase in the airgap length and additional eddy current losses in the steel sleeve, in case of carbon sleeve the cooling problem of magnets arises. So, the rotor must be designed to sustain all mechanical forces coming from defined rotational speeds. It must be pointed out that at the same time the rotor PM excitation in combination with stator electric current must develop torque–speed characteristic as defined in Figure 1.

DRIVEMODE rotor selected technologies/solutions have been: maximum torque defined the rotor outer radius 50 mm, the length 126 mm (including iron fill factor of 0.95), diameter and length smaller than WP1 and WP2 defined space limitations, pole pairs number in accordance to stator design.

DRIVEMODE rotor ferromagnetic material selected technologies/solutions have been: the losses must be as low as possible due to high driving frequencies and the mechanical strength must be high enough to withstand high speeds, the used material in NO20-1200.

DRIVEMODE rotor thermal aspect selected technologies/solutions have been: accordingly to the chosen PM grade (defined by remanent magnetisation) the rotor temperature must be kept in the range below 120 °C.

DRIVEMODE partial or total demagnetization of the PMs selected technologies/solutions have been: higher working temperatures define the temperature dependant demagnetisation, so the chosen PM grade is BMN-42UH/ST.

3.5. Air-gap

- In the case of induction machine the air-gap must be reduced as much as possible. In the case of small air gap the stator magnetizing current become smaller and with this the frequency inverter Volt-Ampere rating is reduced. Mainly, the air-gap thickness is limited by the manufacturing technology.
- When using PMSM the air-gap length depends on the desired level of magnetic flux density in the air-gap. This influences the stator induced voltage, peak torque, nominal and maximum speed and the amount of used PM material.

DRIVEMODE air-gap selected technologies/solutions have been: according to manufacturing technology the air gap length was defined as 0.8 mm, as well as due to PMSM air gap influence on performance characteristics.

3.6. Shaft

The shaft diameter is mainly defined by the maximum value of produced electromagnetic torque. The diameter must be thick enough to sustain the torque which is transferred from e-machine to the gear-box and back (generator operational mode) with some safety factor.



The capacitive coupling between stator windings and rotor structure exist and due to high dV/dt of supplied voltage the electric potential of rotor can increase. At certain rotor potential level the electric discharge currents may occur in the bearings. If the capacitive coupling is not omitted, the bearing currents may also occur in the gearbox via rotor of electric machine. To avoid these, a special ceramic bearings should be used, or specially designed carbon fibre based brushes shall be used to avoid the rise of rotor's and gearbox's electric potential.

DRIVEMODE shaft and bearing selected technologies/solutions have been: the shaft diameter of 35 mm was defined accordingly to transmittable torque over the shaft to the gear box, the bearings have to sustain maximum torque (110 Nm) of the electric machine and the rotor maximum speed (21000 rpm), special ceramic bearings should be used, or specially designed carbon fibre based brushes will be used to avoid the rise of rotor's and gearbox's electric potential.

3.7. Stator housing

The cooling properties of the machine mainly depend on housing type. A high power density e-machines requires the liquid cooling integrated into the stator housing. This is an indirect cooling; it is also possible to arrange direct liquid cooling of the end-windings, as well as, direct in-slot liquid cooling, as these are machine hot-spots. At the IM, the rotor liquid spray cooling is also a choice, on the expense of increased mechanical losses, due to increased friction between coolant and rotating rotor. The combination of all three cooling types is also possible, if the expense is not an issue. The stator housing with cooling ducts with external pump and heat exchanger shall be a moderate choice.

DRIVEMODE stator housing selected technologies/solutions have been: the liquid cooling system integrated into the stator housing with the possibility of direct liquid cooling of the one side (non-drive side) of end-windings.

3.8. E-machine control

The performance of IM as well as of PMSM can be improved by properly controlling them. There exist many control algorithms, but in our case, the most suitable and performance improving is by applying field oriented control (FOC) with implemented maximum torque per ampere (MTPA) motor control algorithm. Above the nominal rotational speed the flux weakening control algorithm is used. Battery voltage shall be transformed by using sinusoidal space vector pulse width modulation (SVPWM). The proposed control algorithms shall be used already in the design and optimisation phase.

DRIVEMODE E-machine control selected technologies/solutions have been: field oriented control (FOC) with implemented maximum torque per ampere (MTPA) motor control algorithm, above the nominal rotational speed the flux weakening control algorithm, all with the sinusoidal space vector pulse width modulation (SVPWM) approach.



3.9. Rotor skewing

The aim of the rotor skewing is to reduce cogging and pulsating torque. Stator or rotor can be skewed, depends on available technology and economics. The rotors are mostly used for this. The torque in function of time is firstly calculated in 2D and then a rotor is divided into the appropriate number of segments. Regarding the curve shape of time dependent torque the segments are shifted to each other for a certain geometric angle. In PMSM rotors the rotor is mostly divided into 2, 3, 4, 5 or 6 segments. This depends on the torque curve shape and the rotor axial length. Meanwhile, the rotor in IM is continuously skewed.

DRIVEMODE rotor skewing selected technology/solution has been: the rotor divided into the six segments for a certain geometric angle.

3.10. Parasitic effects

- **Stator electrical steel sheet**
The eddy current losses shall be omitted by 0.2 mm thin sheets. The hysteresis losses shall be diminishing by using high quality electrical Si based iron. The cutting effect shall be reduced by using punching or in laser cutting technique. The later one is not so good solution from the magnetic point of view, but in the case of prototype is still a good solution. It is expected that stator teeth magnetic properties will be reduced.
- **Rotor electrical steel sheet**
The magnetic flux density in rotor of PMSM is constant with superimposed ripple due to stator teeth reluctance variation and PWM stator currents. The thin rotor lamination steel (the same as in stator) will cancel the additional losses due to flux ripple. In the case of IM, the magnetic flux density in rotor has very low frequency (few percent of driving frequency) and the iron losses can be in some cases neglected.
- **Stator winding**
The stranded coil conductor coil shall be used to reduce skin effect. The conductor diameter depends on the skin effect depth of penetration. To avoid proximity effect and slot leakage flux density effect the stranded conductors' transposition may be used. In the case of hair-pin winding the skin effect depth of penetration must be taken into consideration as well as conductor transposition.
- **Rotor windings**
The main problem may occur, due to mechanical assembly in the case of high rotational speeds.
- **Permanent magnets**
The induced eddy currents, due to magnetic flux density pulsations inside the rotor structure, shall be reduced by permanent magnet segmentation and each segment electrical insulation.
- **End sheet eddy currents**
 - **No-load condition**



In Figure 23, Figure 24, and Figure 25 we can see the distribution of magnetic flux density almost (0.1 mm above) on the stator end-sheet surface. The circular stator form was transformed into perpendicular plane. The zero plane level represents the near stator surface. The positive and negative distributions show the values of magnetic flux density normal component B_z in z-direction (along the machine axis) on the stator end-sheet. There can be seen the stator slots (low level of B_z) and the teeth regions (high level of B_z). In the no-load condition the maximum value of B_z is in the range of 0.35 T. The rate of change of B_z depends on rotor rotational speed. It can be expected quite high iron losses in the both stator end-sheet surfaces.

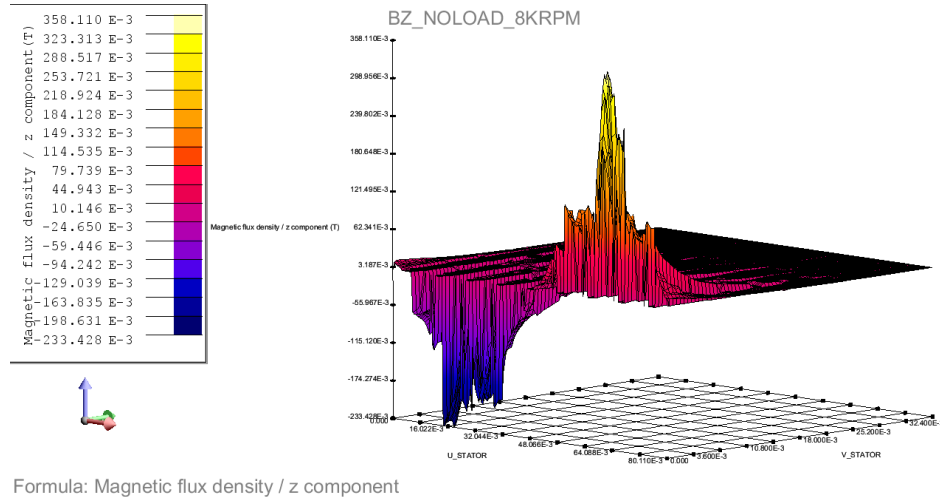


Figure 23 Magnetic flux density normal component B_z (in z-direction, along the machine axis) distribution at no-load conditions almost (0.1 mm above) on the stator end-sheet surface

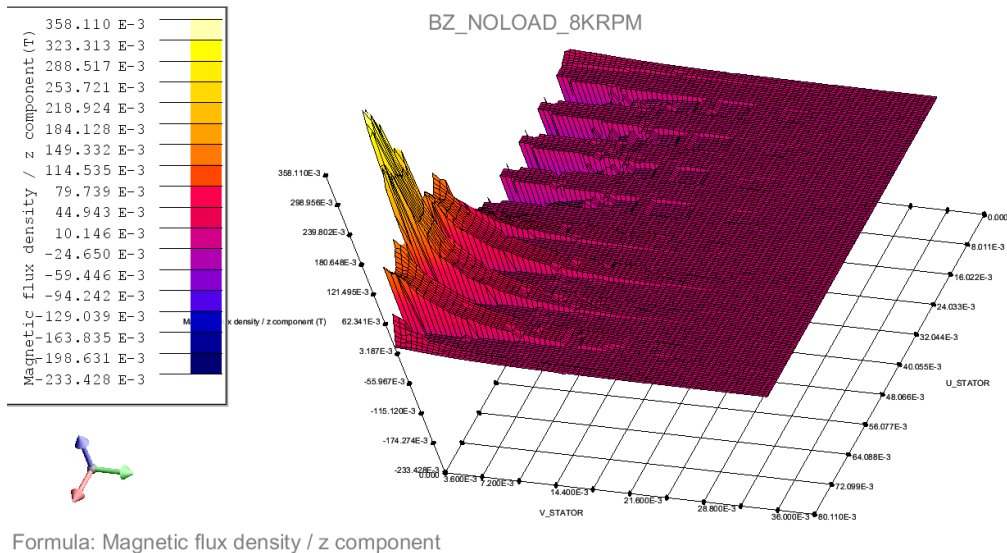


Figure 24 Magnetic flux density normal component B_z (in z-direction, along the machine axis) distribution at no-load conditions almost (0.1 mm above) on the stator end-sheet surface



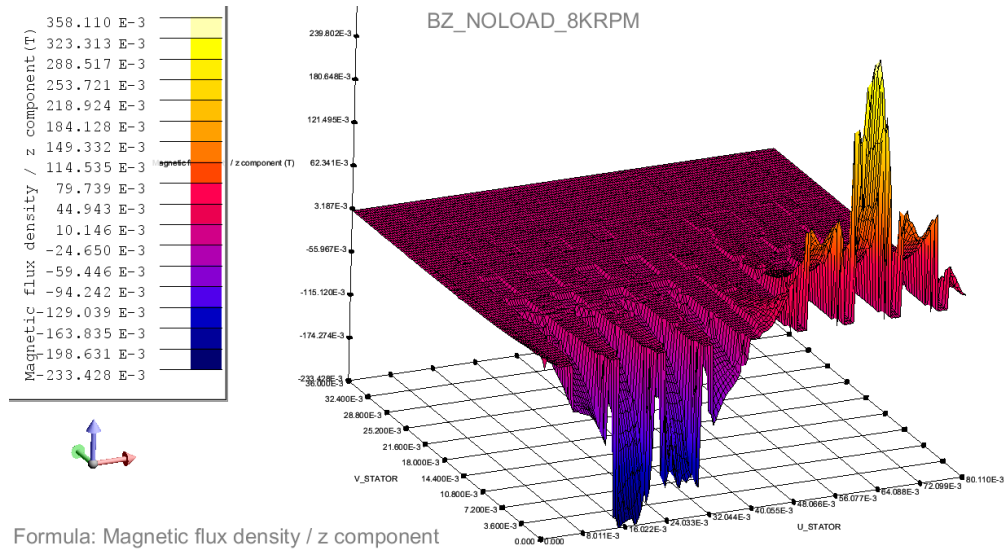


Figure 25 Magnetic flux density normal component B_z (in z-direction, along the machine axis) distribution at no-load conditions almost (0.1 mm above) on the stator end-sheet surface

- Load condition

In Figure 26 and Figure 27 we can see the distribution of magnetic flux density almost (0.1 mm above) on the stator end-sheet surface. The circular stator form was transformed into perpendicular plane. The zero plane level represents the near stator surface. The positive and negative distributions show the values of magnetic flux density normal component B_z in z-direction (along the machine axis) on the stator end-sheet. There can be seen the stator slots (low level of B_z) and the teeth regions (high level of B_z). In the load condition the maximum value of B_z is in the range of 1 T. The level depends on the value of applied stator currents and stator current weakening angle. The final distribution of B_z is the combination of no-load B_z due to PM and B_z due to applied stator currents at certain stator current flux weakening angle. The rate of change (flux fluctuation like a waves) of B_z depends on rotor rotational speed. It can be expected very high iron losses in the both stator end-sheet surfaces.



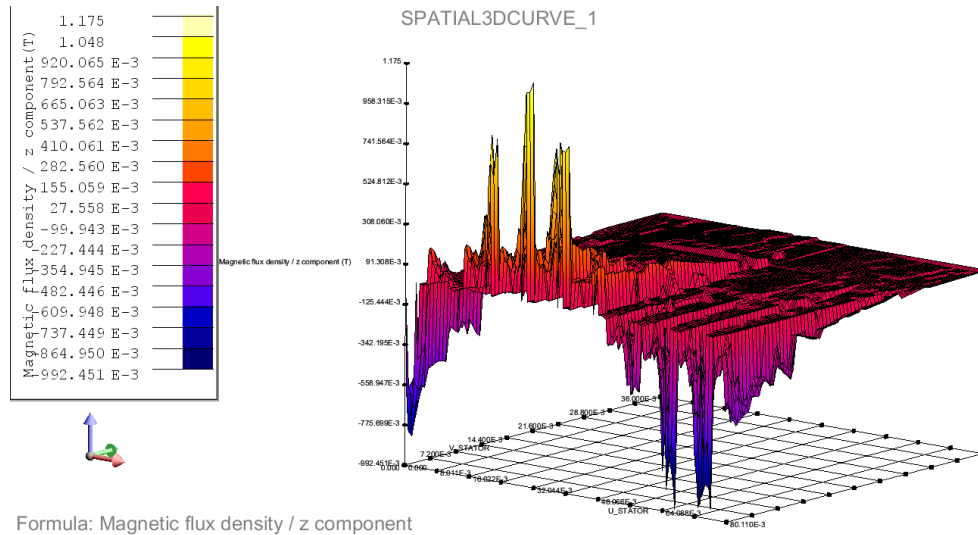


Figure 26 Magnetic flux density normal component B_z (in z-direction, along the machine axis) distribution at load conditions almost (0.1 mm above) on the stator end-sheet surface

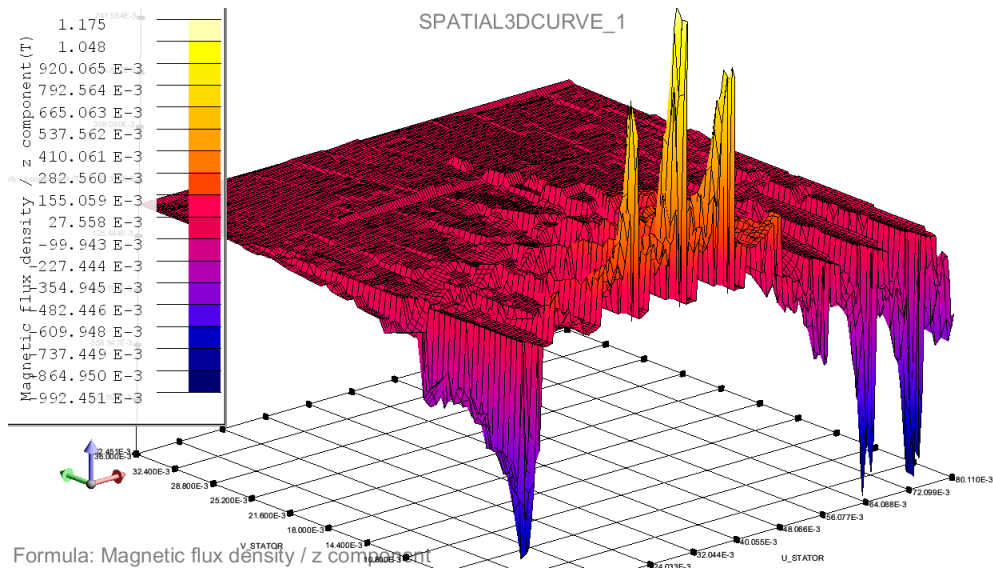


Figure 27 Magnetic flux density normal component B_z (in z-direction, along the machine axis) distribution at load conditions almost (0.1 mm above) on the stator end-sheet surface

One of the solutions is to apply the ferrite material (electrically nonconducting material) on the end-sheet surface of stator teeth to by-pass (to re-direct) the magnetic flux density normal component B_z from stator lamination (NO20 material) to ferrites. The ferrite material has much lower iron losses at higher frequencies in comparison to NO20. Ferrite material is a composite material – no preferred direction to guide magnetic flux density and this give us a possibility to guid the magnetic flux in all 3 dimensions.. Also, there is also a solution to have a stator package longer then rotor package, but this solution is a waste of material.



4. Calculation Methodology

There were used different approaches to properly design, calculate and analyses the IM and PMSM. The multi-physical approach was used in 2D and 3D in finite element environment. The performance calculations were interlaced between the electromagnetic, thermal and mechanical analysis. Why interlaced, e.g. a small change in electromagnetic PMSM rotor design can influence the mechanical strength as well as output torque and induced voltage. So, all multi-physical behaviours must be re-calculated to validate the effect of applied change.

4.1. Electromagnetic analyses

- Magneto-static analysis (2D/3D)
This solver is used to analyse magnetic load-ability, cogging torque, inductances, magnetic flux linkage and leakage,...
- Magneto-transient analysis (2D/3D)
The time-dependent solutions are studied by applying this analysis. The results are: induced voltages, torque in function of time, torque pulsations, iron losses, copper losses, magnetic saturations....
- Electric circuit and magneto-transient analysis coupling (2D/3D)
By applying this analysis the influence of control strategy as MTPA and flux weakening are involved in design and optimization.
- Steady-state AC analysis (2D/3D)
This approach is used in IM analyses, design and optimization. The results are: torque versus speed (slip), stator and rotor currents vs. speed (slip), shaft power vs. speed (slip), iron and copper losses,....

4.2. Thermal analyses

- Steady state thermal analysis (2D/3D)
The final temperature distribution in whole e-machine is calculated for different losses and cooling types.
- Transient thermal analysis (2D/3D)
The temperature distribution in time in whole e-machine is calculated for different losses and cooling types. This approach allows studying the machine over-load-ability as a losses and temperature are time dependent.

4.3. Mechanical analyses

- Static structural analysis (2D)



The mechanical properties are calculated by applying this solver. The mechanical stress distribution over all rotor structure is analyzed and optimized at different rotational speeds (maximum, spinning and burst speeds) .



5. Concepts results

5.1. PMSM V2a results

The PMSM V2a machine is a three phase machine with 36 slots stator and 8 poles rotor. The achievable output electrical properties are shown in Table F. The mechanical properties of PMSM V2a presented in Table G and Table H. The electrical steel material properties for stator and rotor used in machine design and iron losses calculation is M270-35A, but the prototype will be produced from electrical steel NO20-1200 with significantly improved performance, especially are reduced iron losses. So, the iron losses in prototype are to be expected lower and the overall better efficiency.

Table F Electromechanical performance at peak operational conditions for PMSM V2a

PEAK PERFORMANCE					
n (rpm)	50	7000	10000	15000	20000
T (Nm)	106.3	106.4	72.4	43	31
I _{ph,rms} (A)	140	140	115	95	85
alpha (deg)	45	45	61	70	75
U _{ph,max} (V)	10.9	391.2	413.4	410.2	413.2
P _{mech} (kW)	0.6	78.0	75.8	67.5	64.9
Tripple (Nm), peak-to-peak	6.50	6.52	6.32	4.37	3.80

Table G Mechanical properties of PMSM V2a

	regular W N=3turn/slot/phase	
DIMENSIONS		
Outer stator diameter	174.00	mm
Inner stator diameter	102.00	mm
Air gap width	1.00	mm
Outer rotor diameter	100.00	mm
Shaft diameter	40.00	mm
Active length	140.00	mm



	regular W N=3turn/slot/phase	
Stator-yoke thickness	11.00	mm
Stator-tooth width	5.00	mm
Stator-tooth length	23.30	mm
Stator pole shoe (h_ds1)	0.70	mm
Stator pole shoe (h_ds2)	1.00	mm
Slot opening	2.10	mm
WINDING		
Number of stator slots	36	
Number of pole pairs	4	
Number of slots per pole per phase	1.5	
Number of layers	2	
Number of coils per pole pair per phase	3	
Number of series turns per coil	3	
Number of series turns per phase	36	
Stator slot fill factor	0.33	

Table H Masses of different PMSM V2a machine parts and total mass

MASSES OF THE PMSM V2a PARTS	Lfe=140mm Dr=100mm TO BE USED FOR COMPARISON	
Stator iron	11.20	kg
Winding	4.40	kg
Rotor iron	5.70	kg
Magnets	1.50	kg
Shaft	1.1	kg
Total	23.90	kg



The applied permanent magnet properties are presented in Table I Properties of applied permanent magnets.

Table I Properties of applied permanent magnets

Remanent flux density at 20 °C	1.37	T
Remanent flux density at 100 °C	1.25	T
Relative permeability	1.05	
Intrinsic coercive field strength at 100 °C	min. 800-1000	kA/m
Suggested magnet grade	BMN-42UH/ST	

Maximum achievable torque at given electrical, magnetic and mechanical boundaries is presented in Figure 28 Peak torque speed curve for PMSM V2a. As it can be seen the performance goal as defined in general performance requirements is achieved in all region.

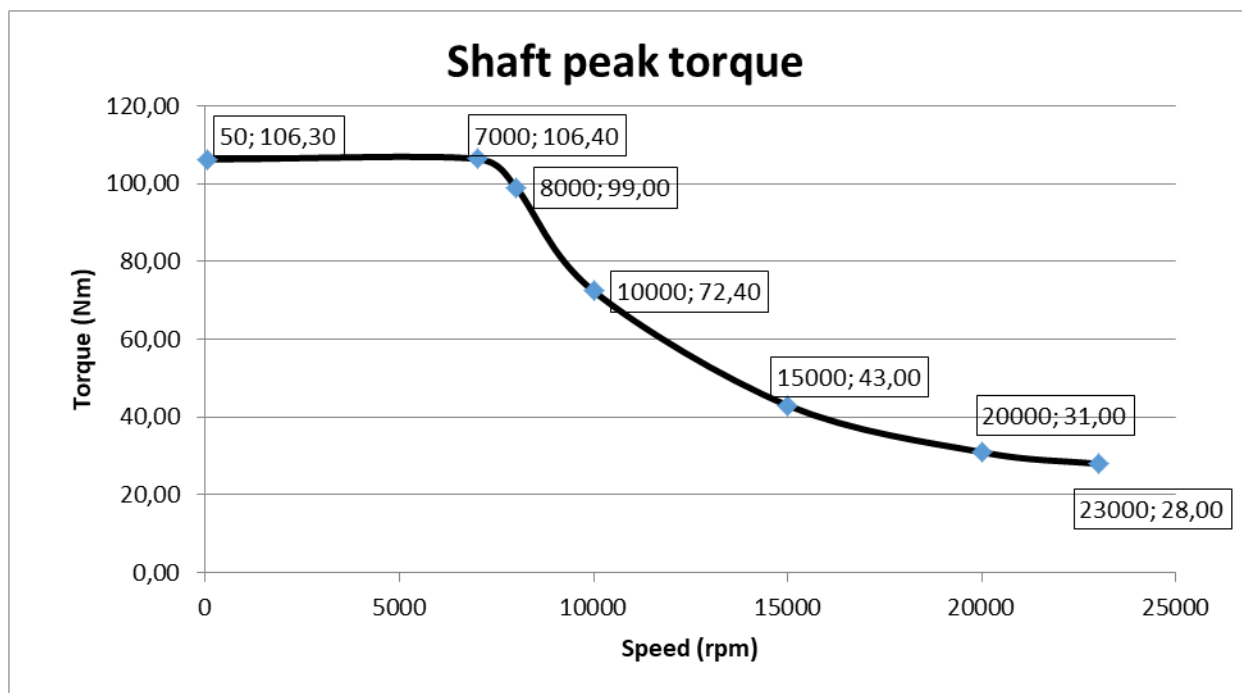


Figure 28 Peak torque speed curve for PMSM V2a

The peak power versus speed curve for PMSM V2a is given in Figure 29.



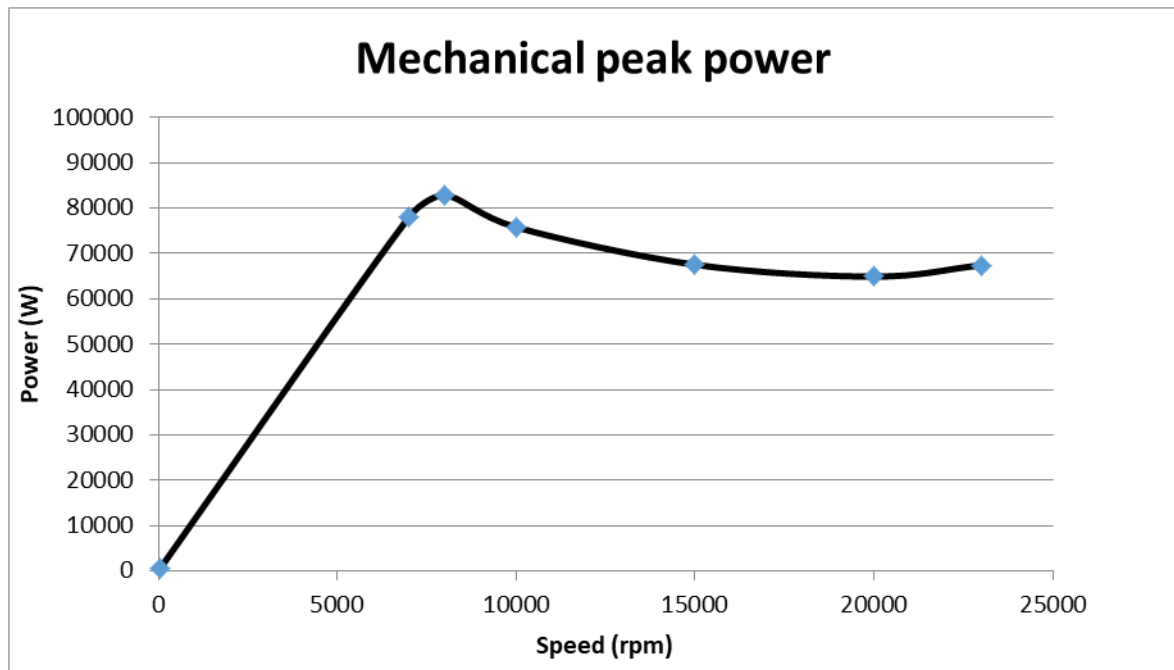


Figure 29 Peak power versus speed curve for PMSM V2a

The efficiency curve for peak operational points at 130 °C are shown in Figure 30.

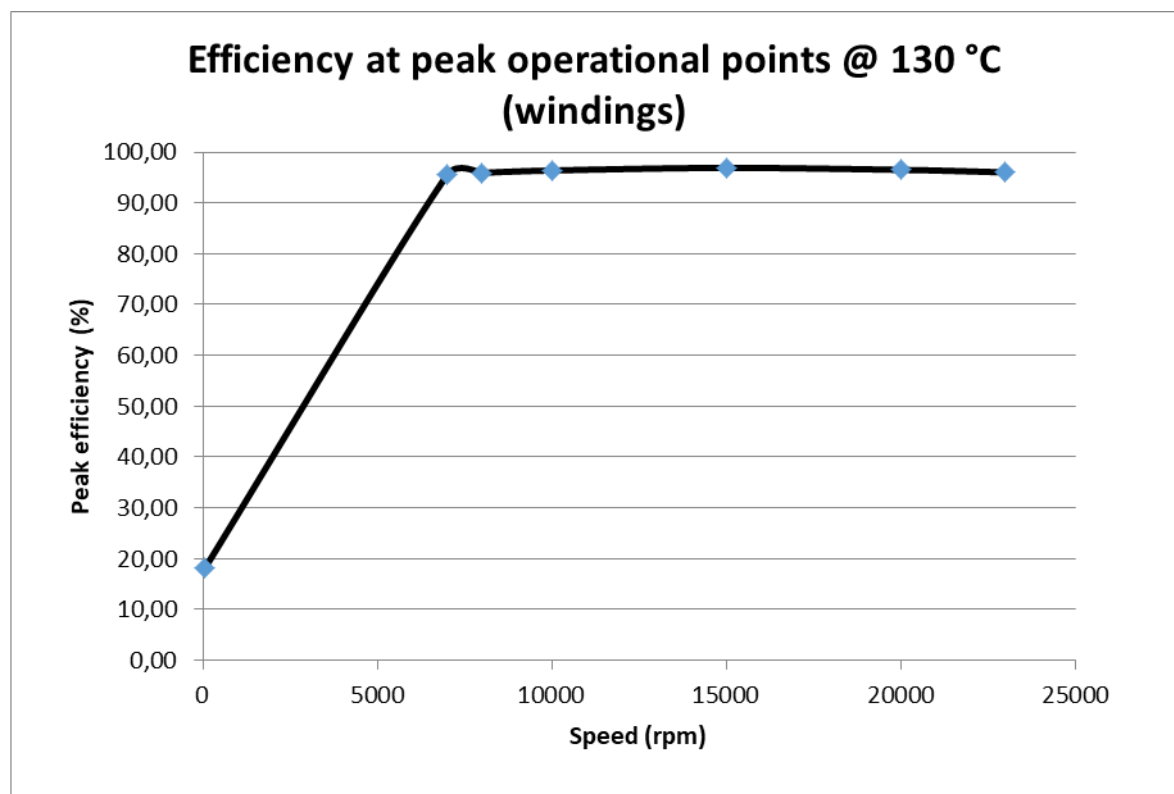


Figure 30 Efficiency curve for peak operational points at 130 °C



The efficiency map of PMSM V2a is presented in Figure 31.

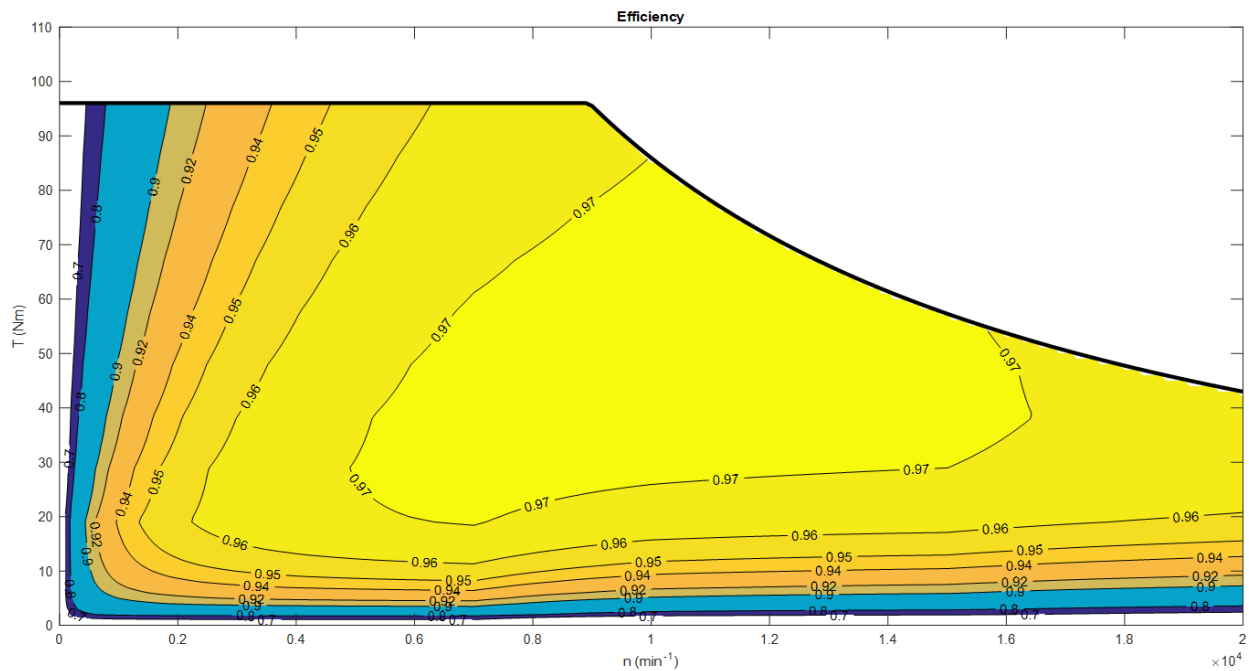


Figure 31 Efficiency map of PMSM V2a

Working points for PMSM performance evaluation and comparison are presented in Table J. Phase voltage amplitude of 410 V corresponds to 720 V dc battery, which is the lowest (still under consideration with project partners) allowed battery voltage (nominal battery voltage is 800 V).

Table J Working points for PMSM performance evaluation

Speed [rpm]	Torque [Nm]	Irms (A)	Uamp_phase (V)	cos(θ)	Efficiency (%)	Frequency (Hz)
762	5	11	24	0.84	88.7	50.80
2402	12	19	75	0.88	95.2	160.13
2768	24	34	88	0.9	96.2	184.53
3279	36	50	125	0.95	96.3	218.60
5570	4	7	175	0.94	91.1	371.33
6058	11	17	186	0.95	95.8	403.87
6237	21	32	196	0.95	97	415.80
9525	6	11	288	0.93	91.6	635.00
10529	14	24	308	0.95	95.6	701.93
13320	21	34	408	0.95	96.6	888.00



Thermal behaviour of PMSM V2a (Fig. 31) is studied in transient state at continuous operational mode. The temperature distribution is calculated for different machine parts. These temperature results are presented in Fig. 32. The temperature changes at overload (peak power) operation for 60 seconds with starting temperature 100 °C is shown in Fig. 33.

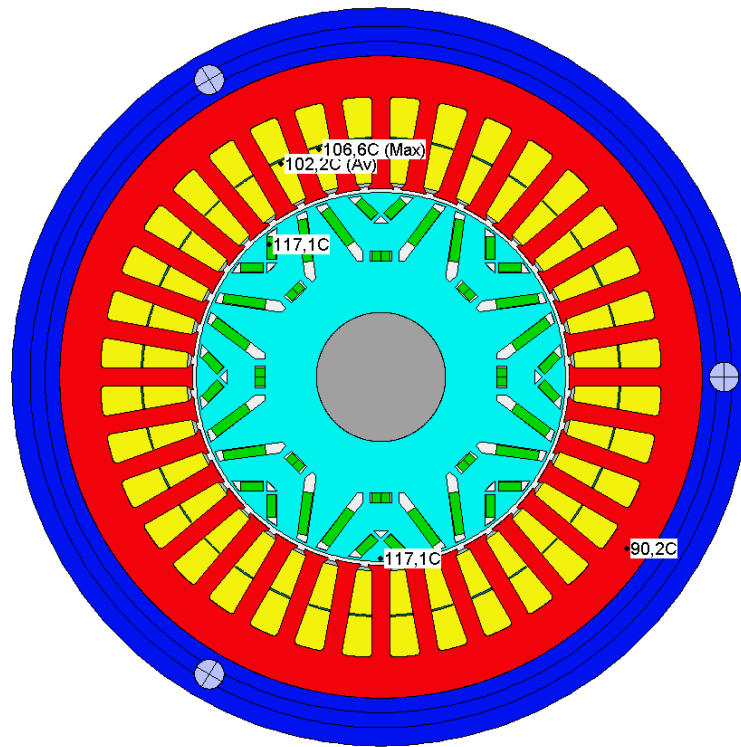


Figure 32 PMSM V2a cross section for thermal study

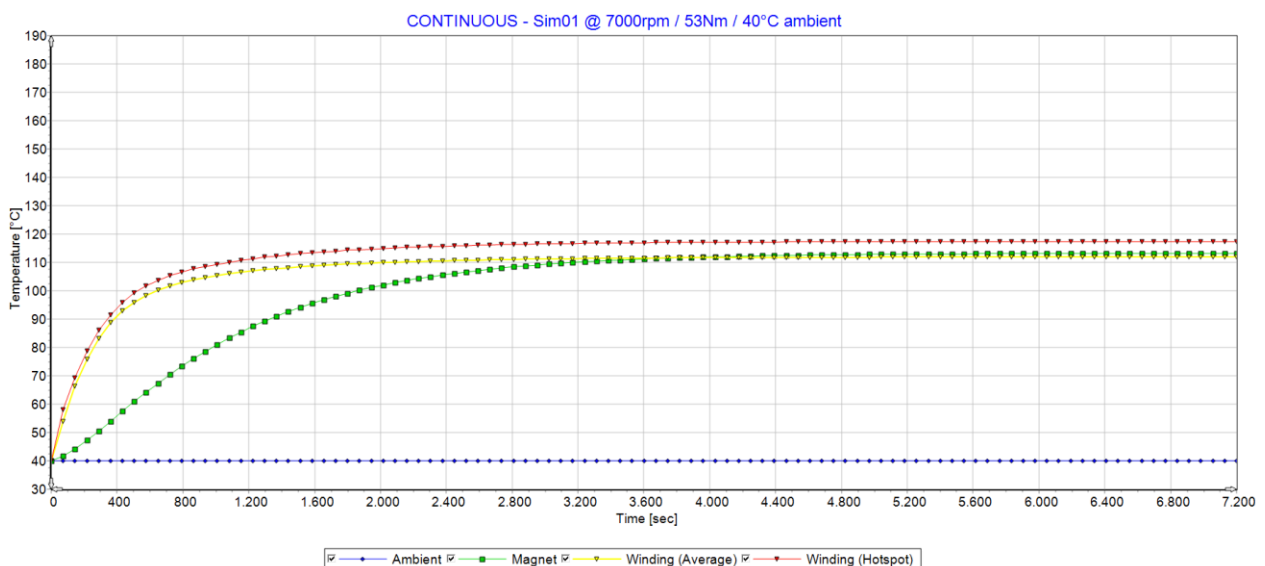


Figure 33 Temperature rise in different machine part during continuous operational mode



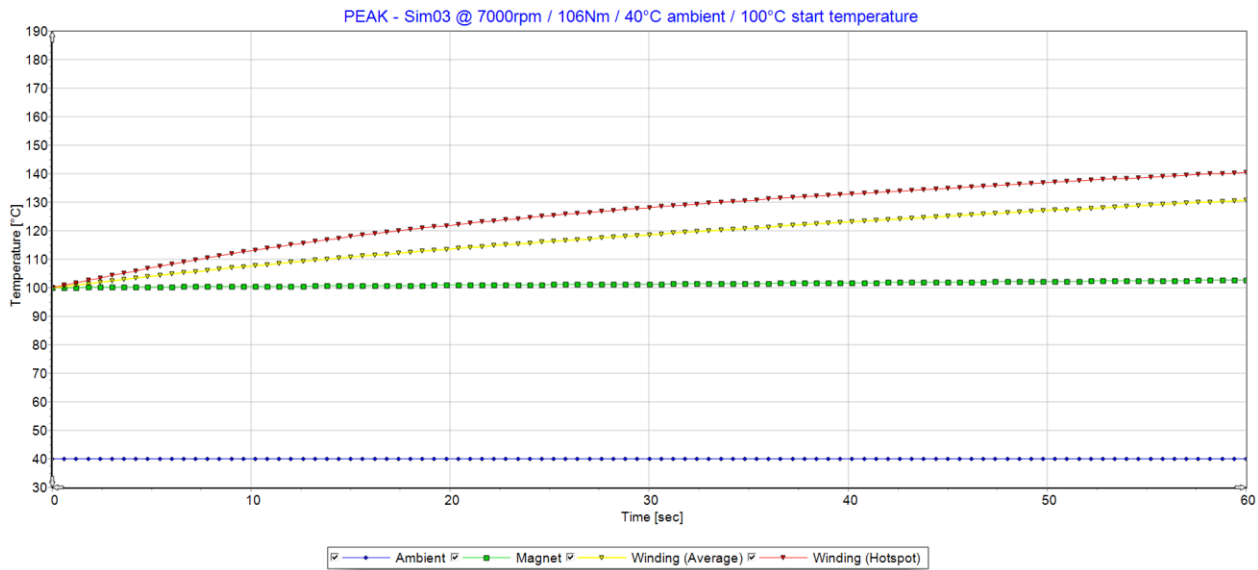


Figure 34 Temperature rise in different machine part during peak power operational mode for 60 seconds at ambient temperature 100 °C

The PMSM design is still in progress with the main goal to reduce machine outer dimensions, while keeping the performance at general performance requirements level.

5.2. IM V5a results

The IM V5a is a three phase machine is a 4 pole machine with 36 stator slots and 46 rotor slots. The achievable output electrical properties are shown in Table K. Maximum achievable torque at given electrical, magnetic and mechanical boundaries is presented in Figure 35 in comparison to the general performance requirements.

Table K Characteristic operation points IM of IM V5a

Operation points	Unit	Cont. 1	Cont. 2	Peak 1	Peak 2	Peak 3
Speed	rpm	7086	20000	7086	20000	13500
Torque	Nm	47.17	15.93	106.78	15.93	30.30
Current, line	A _{rms}	46.8	44.1	110	44.1	64.7
Power, mech.	kW	35	33	79	33	43
Torque ripple p2p	Nm	3.50	2.30	13.50	2.30	2.50
Efficiency	%	95.6	91.2	93.6	91.2	91.8



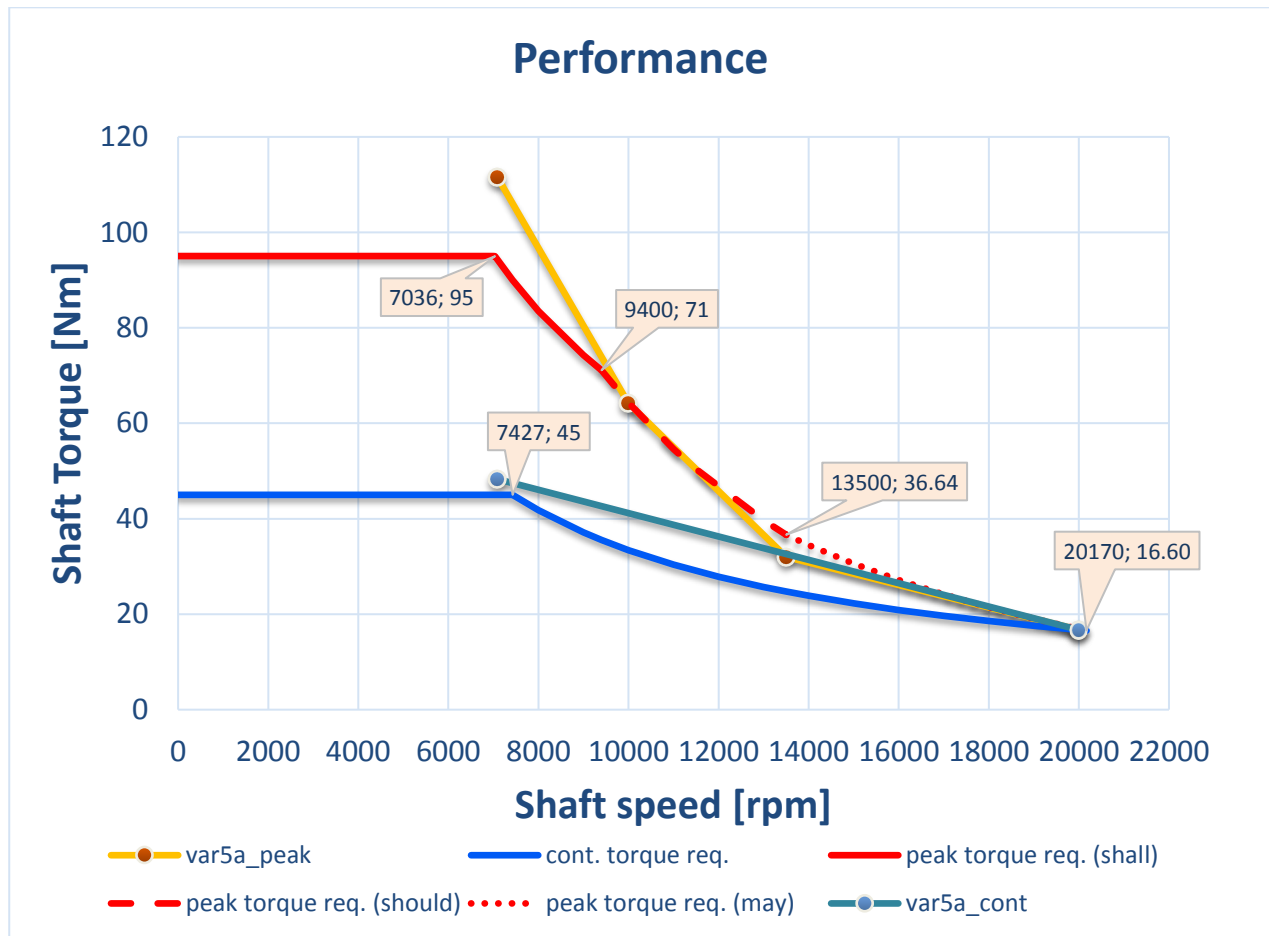


Figure 35 Torque speed-characteristics of designed and evaluated induction machine Var5a

The mechanical properties of IM V5a are presented in Table L and Table M. The rotor cage material is copper. The electrical steel material properties for stator and rotor used in machine design and iron losses calculation is NO20-1200.

Table L Dimensions of IM V5a

Item	Unit	Value
Number of Poles		4
Number of Stator Slots		36
Housing outer diameter	mm	260
Stator outer diameter	mm	210
Stator inner diameter	mm	144
Airgap width	mm	0.5
Rotor outer diameter	mm	143
Rotor inner diameter	mm	35



Table M Weight of IM V5a

Item	Unit	Value
Stator Copper	kg	5
Stator Lamination	kg	17
Rotor Lamination	kg	14
Magnet	kg	0
Rotor Cage	kg	3.6
Insulation	kg	0.5
Total weight active parts	kg	40.1
Rotor volume	l	2.29

Working points for IM performance evaluation and comparison are presented in Table N. Phase voltage amplitude of 410 V corresponds to 720 V dc battery, which is the lowest (still under consideration with project partners) allowed battery voltage (nominal battery voltage is 800 V)

Table N Working points for IM V5a performance evaluation

Speed (rpm)	Torque (Nm)	Current (Arms)	Voltage (Vrms)	Power Factor	Efficiency (%)
762	1.8	39.5	38.9	0.143	14.78
2402	11.3	29.2	113.1	0.316	86.66
2768	25.8	33.7	130.8	0.595	92.46
3279	41.0	40.4	148.5	0.814	93.73
5570	6.2	19	232.6	0.282	89.94
6058	13.4	21.9	253.1	0.521	94.55
6237	21.0	25.8	261.6	0.689	95.71
9525	6.0	13.1	293.9	0.523	94.16
10529	15.9	20.3	293.9	0.987	97.06
13320	21.3	36.5	293.9	0.937	95.73

Thermal behaviour of IM V5a (Figure 36) under nominal cooling conditions is studied in transient state at continuous operational mode. The temperature distribution is calculated for different machine parts. These temperature results for characteristic loads out of the continuous



operating region are presented in Figure 37 and Figure 38. The temperature changes at overload (peak power) operation for 60 seconds with starting temperature 100 °C is shown in Figure 39.

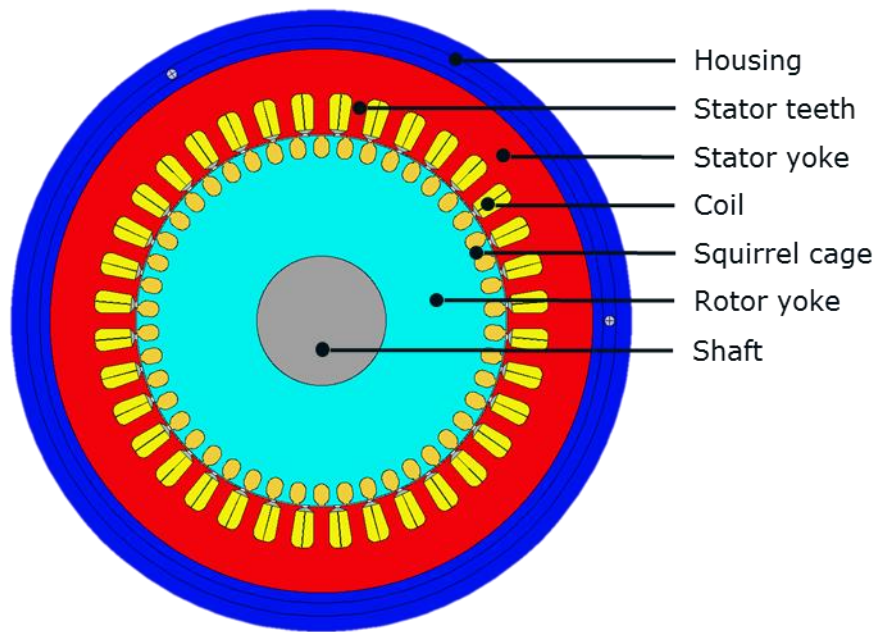


Figure 36 IM V5a cross section for thermal study

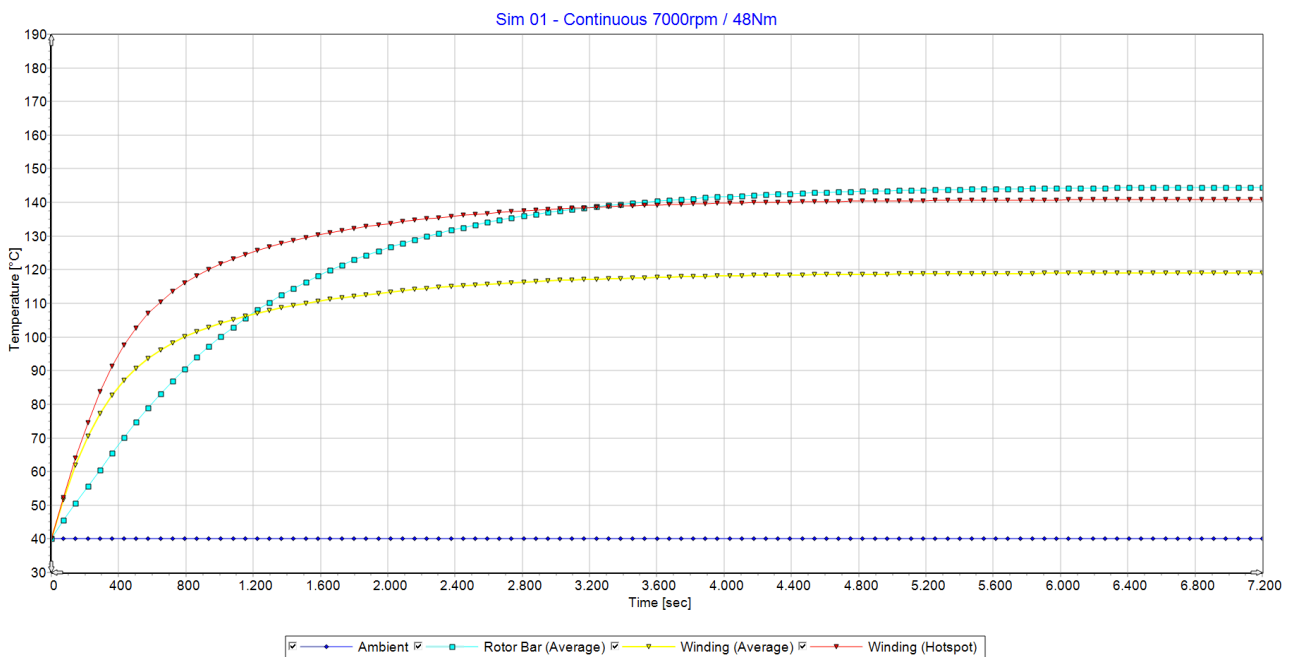


Figure 37 IM V5a: Temperature rise in different machine part during continuous operational mode



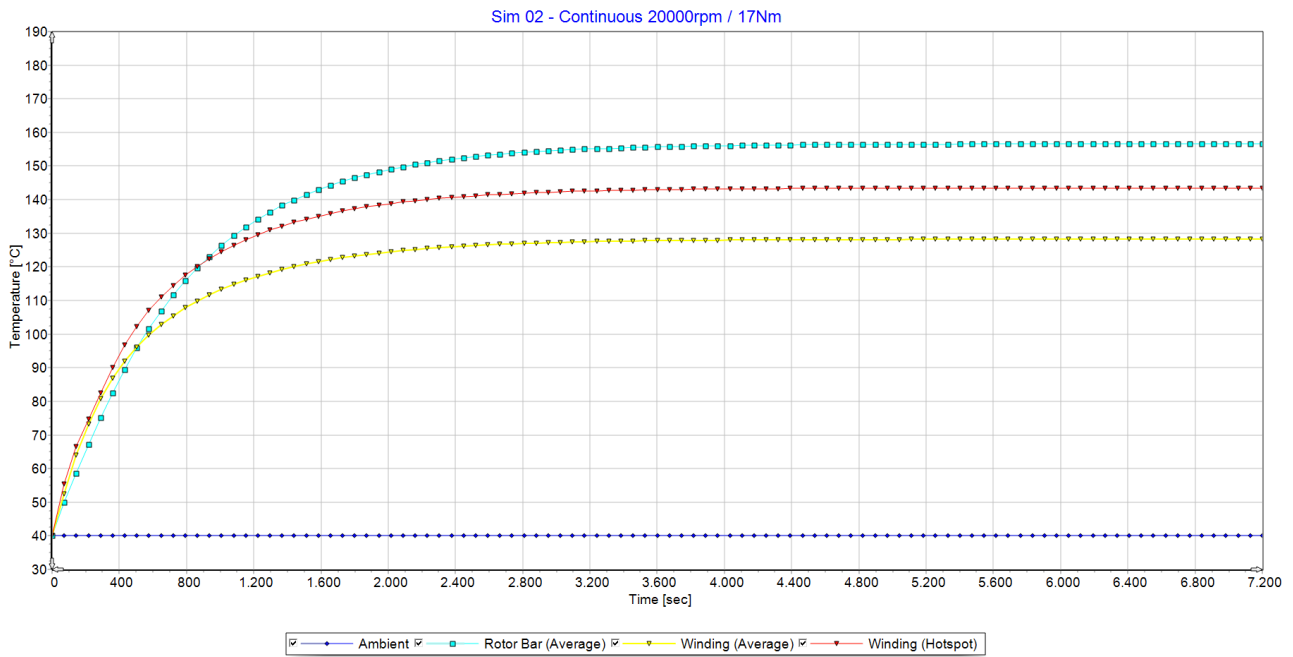


Figure 38 IM V5a: Temperature rise in different machine part during continuous operational mode at maximum speed

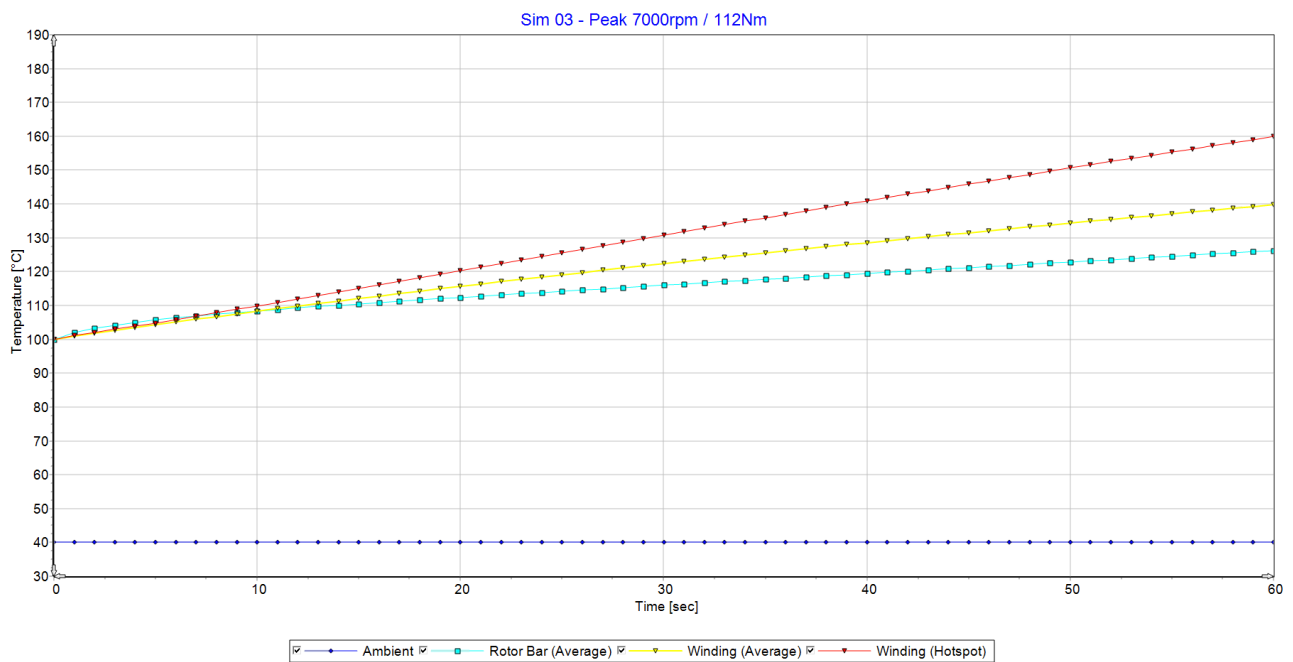


Figure 39 IM V5a Temperature rise in different machine part during peak power operational mode for 60 seconds at ambient temperature 100°C



6. Evaluation matrix

The DRIVEMODE project partners used multi-attribute utility theory, (MAU) and derivatives method for decision-making. Based on this theory the evaluation matrix was established and the results are shown in Table N. The performance comparison was done between Induction machine Var05b and Permanent magnet synchronous machine Var 02b. The difference between Permanent magnet synchronous machine Var 02a and Var2b is just in the concept of hair-pin winding. With this concept we achieved better copper fill factor.

Table O Weighted Decision Matrix -DriveMode Concepts

Criteria Description			Weighting		Ranking		Weighted Ranking	
					E-Motor		E-Motor	
Evaluation Criteria	Explanation	Additional information	Assigned	Computed	Var05b (ASM)	Var02b (PM)	Var05b (ASM)	Var02b (PM)
Compactness		Based on "Total volume" Var02b: 19.9kg Var05b:27.3 kg ⁽¹⁾	3.00	0.143	2	1	0.286	0.143
Peak efficiency			1.00	0.048	2	1	0.095	0.048
Robustness			1.00	0.048	1	2	0.048	0.095
Weight		Based on "total weight of active parts" Var02b: 19.9kg / Var05b: 27.03kg ⁽¹⁾	2.00	0.095	2	1	0.190	0.095
Resource availability	Recyclability	Based on usage of rare earth materials	3.00	0.143	1	2	0.143	0.286
			21.00	1.000			0.76	0.67

Table O explanation.

Weight assigning to criteria (wi): the weights serve as scaling factors to specify relative importance of each criterion.

Since weights are scaling factors specifying relative importance in the overall set of criteria, they should be non negative numbers that sum to 1. We used the following categories for weighting the criteria from low importance to high importance as follows:

- H means "High importance" – value 3
- M means "medium importance" – value 2
- L means "low importance" – value 1

 Winning concept



This project has received funding from the European Union's Horizon 2020 research and innovation programme under grant agreement N° 769989.

 **DRIVEMODE**



Loosing
concept

¹⁾ "WP3 E-Motor Concept Design Status_20180706_kwa_01.pdf"

[<https://drivemode.cloud.icube.global/index.php/f/6380>] created by Katrin Wand AVL

Comments:

Note on method

Using multi-attribute utility theory, (MAU) and derivatives method for decision-making.

The MAU method is a model that: 1) Incorporates input from the various stakeholders in the decision; 2) Identifies the factors that are important in the decision and the alternative decision options; 3) Weights the factors; 4) Ranks the alternative decision on how well they serve the factors; 5) Provides an overall score that identifies the best options.

By convention in MAU analysis, any scoring function should be normalized for the scores to fall in the range of 0 to 1

Benchmark :

Our chosen concept of PMSM machine can be compared to other presented automotive main electrical machine. The presentation is shown in Table P.

Table P Comparison between different automotive main electrical machine

Power density	2012 Leaf (80 kW)	2011 Sonata (30 kW)	2010 Prius (60 kW)	2008 LS600h Lexus (110kW)	2007 Camry (70 kW)	2004 Prius (50 kW)	DRIVE MODE 80kW	2016 BMW i3 Motor (125 kW)
kW/kg	1.4	1.1	1.6	2.5	1.7	1.1	3.4*	3.8

- * still under optimisation, the goal is to achieve power density of 4.7 kW/kg (active mass, at $140A_{eff}$, at permanent magnet temperature $90^{\circ}C$ and $800V_{dc}$ (fully charged battery)) and in terms of higher available currents 220A, at permanent magnet temperature $120^{\circ}C$ at battery voltage of $800V_{dc}$ the power density of 6 kW/kg (active mass) or 4.5 kW/kg (total mass).



7. Concept decision

The DRIVEMODE project partners decide that the PMSM V2a is accepted as a design to be used as main traction machine concept (see section Evaluation Matrix). It has to be pointed out, that the partners advise to further optimise the PMSM. Mainly in reduction of machine volume and mass (reduction in used material) while keeping the performance at the same level. And also, to improve the overall efficiency of the proposed PMSM design as well as, to improve efficiency at the proposed working points (as the drive system performance check).

Further development, design and analyses will go in minimisation of material consumption, improved over-load-ability (in the case of higher available frequency inverter currents), increase of overall efficiency, increase of efficiency in working points (Table O), definition of proper skew angle (number of segments), detailed thermal modelling and cooling system improvement. The PMSM mechanical behaviour will be analysed in terms of separate machine parts resonance frequencies of, as well as whole system. The overall drive train (gear box, PMSM and power inverter) will be analysed in terms of noise and vibrations.



8. Conclusions

The document as the deliverable D3.2 “Report on considered electrical motor technologies, evaluation matrix, and concept decision” summarises the E-Machine functional requirements and presents the E-machines benchmark applied in electric vehicles and industrial applications through the literature overview. In the section “Considered electric motor technologies” there are presented in detail the basic e-machine components and the approaches for their design as well as, the possible problems and drawbacks during the design and development. Different types of material are also introduced and analysed. The effects of parasitic effect are also explained and the procedures how to overpass them are also proposed. The calculation methodology section explains which analyses should be used to properly calculate and evaluate the e-machine performance.

The two concept designs used during the e-machine development are presented in section “concept design”. They are the Permanent Magnet Synchronous Machine (PMSM) and the Induction Machine (IM) concepts. Some performance results are also gathered in this section.

The DRIVEMODE project partners used multi-attribute utility theory and derivatives method for decision-making and the results are presented in section “Evaluation Matrix”. The result of these analyses and evaluation is a concept selection for further development and application as main propulsion electric machine in DRIVEMODE project, which is PMSM.

This is a document where the evaluated approaches have been presented. All new achievements will be presented in the upcoming reports.



9. References

- [1] Liu, Yujing, and Nimananda Sharma. "Preliminary design of modular drivetrain system." 2018.
- Wand, Katrin. "D3.1 Report on electrical motor requirements." 2018.
- [3] Pia Lindh (Juha Pyrhönen): Multidisciplinary design of a permanent-magnet traction motor for a hybrid bus taking the load cycle into account, 2016
- [4] Liang Chen: Reduced dysprosium permanent magnets and their applications in electric vehicle traction motors, 2015
- [5] Ayman M. EL-Refaie: Advanced high-power-density interior permanent magnet motor for traction applications, 2014
- [6] Kyohei Kiyota: Comparison of test result and design stage prediction of switched reluctance motor competitive with 60 kW rare-earth PM motor, 2014
- [7] Kyohei Kiyota: Design of switched reluctance motor competitive to 60 kW IPMSM in third generation hybrid electric vehicle, 2011
- [8] James R. Hendershot: MotorSolve analysis of the 2010 Toyota Prius traction motor, 2015
- [9] J. Merwerth: The hybrid-synchronous machine of the new BMW i3 and i8, 2014
- [10] Tim Burress: Benchmarking EV and HEV technologies, 2016
- [11] David Staton: Open source electric motor models for commercial EV and hybrid traction motors, 2017
- [12] Tim Burress: Benchmarking state-of-the-art technologies, 2013
- [13] Honda Accord Model Information,
<http://owners.honda.com/vehicles/information/2014/AccordHybrid/specs#mid^CR6F3EEW>, 2018
- [14] Mitch Olszewski: Evaluation of the 2008 Lexus LS 600H hybrid synergy drive system, 2009
- [15] Mitch Olszewski: Evaluation of the 2007 Toyota Camry hybrid synergy drive system, 2008
- [16] Siemens catalogue of several different motors, 2017
- [17] Jingjuan Du: Optimization of magnet shape based on efficiency map of IPMSM
- [18] Jin Hur: Characteristic analysis of IPM synchronous motor in electrohydraulic power steering systems, 2008
- [19] Jiabin Wang: Design optimization of a surface-mounted permanent-magnet motor with concentrated windings for electric vehicle applications, 2013
- [20] Tao Sun: Effect of pole and slot combination on noise and vibration in permanent magnet synchronous motor, 2011
- [21] You-Young Choe: Comparison of concentrated and distributed winding in an IPMSM for vehicle traction, 2012
- [22] Parker catalogue: Electric and hybrid vehicle - Accessory, power generation and traction motor solutions, 2014
- [23] Parker catalogue: GVM Global Vehicle Motor, 2017
- [24] S. Pint, N. Ardey, G. Mendl, G. Fröhlich, R. Straßer, T. Laudénbach, J. Doerr: Audi AG, Wiener Motoren Symposium 2018.
- [25] <https://www.emotor.com/windings/>
- [26] BOMATEC, www.bomatec.ch



10. Appendices

10.1. List of abbreviations

CPSR	constant power speed range
EMAG	electromagnetic simulations
FEM	finite element modelling
FOC	field oriented control
IDM	integrated drive module
IM	induction motor
MTPA	maximum torque per ampere
PDIV	partial discharge inception voltage
PMSM	permanent magnet synchronous machine
PWM	pulse width modulations
SVPWM	space vector pulse width modulation
TBD	to be defined
THERM	thermal simulations

